

Antitumor Activity of New Enantiopure Pybox-Ruthenium Complexes

Estefania Menéndez-Pedregal,^a Josefina Díez,^a Ángel Manteca,^b Jesús Sánchez,^b Ana C. Bento,^c Rosula García-Navas,^c Faustino Mollinedo,^c M. Pilar Gamasa^{*a} and Elena Lastra^{*a}.

^[a] *Departamento de Química Orgánica e Inorgánica, Instituto de Química Organometálica “Enrique Moles” (Unidad Asociada al C.S.I.C.). Universidad de Oviedo, 33006 Oviedo, Principado de Asturias, Spain.*
E-mail: elb@uniovi.es (E. Lastra).

^[b] *Departamento de Biología Funcional, Instituto Universitario de Biotecnología de Asturias, Área de Microbiología. Universidad de Oviedo, 33006 Oviedo, Principado de Asturias, Spain.*

^[c] *Instituto de Biología Molecular y Celular del Cáncer, Centro de Investigación del Cáncer, CSIC-Universidad de Salamanca, Campus Miguel de Unamuno, E-37007 Salamanca, Spain.*

- **Experimental data for complexes 1c-7c.**
- **Selected NMR spectra:** ¹H, ³¹P{¹H}, ¹³C{¹H}, DEPT 135 and selected bidimensional NMR experiments COSY HH, HSQC and HMBC spectra for complexes **1a**, **2a**, **3a**, **5a**, **1b**, **2b**, and **6c**.
- **Antimicrobial Activity.**
Experimental, Table 1 and Figure 1.
- **Crystal and refinement data for complexes 1b, 2a·CH₂Cl₂ and 3b (Table 2)**

Experimental data for complexes 1c-7c.

trans-[RuCl₂{(*R,R*)-^{*i*}Pr-pybox}(PTA)] (1c):

Yield: 0.397 g, 90%. S_{293 K} (H₂O): 31.40 mg/mL. ¹H NMR (300.13 MHz, CD₂Cl₂, 298 K) δ 7.81 (m, 3H, H^{3,4,5} C₅H₃N), 4.85–4.69 (m, 10H, OCH₂ and NCH₂N), 4.56 (m, 6H, NCH₂P), 3.97 (m, 2H, CH^{*i*}Pr), 2.27 (m, 2H, CHMe₂), 1.07 (d, ³J_{HH} = 7.6 Hz, 6H, CHMe₂), 0.72 (d, ³J_{HH} = 6.4 Hz, 6H, CHMe₂) ppm. ¹³C{¹H} NMR (100.61 MHz, CD₂Cl₂, 298 K) δ 164.9 (s, OCN), 147.6 (s, C^{2,6} C₅H₃N), 133.0 (s, C⁴ C₅H₃N), 122.7 (s, C^{3,5} C₅H₃N), 73.6 (d, ³J_{CP} = 6 Hz, NCH₂N), 72.4 (s, CH^{*i*}Pr), 71.1 (s, OCH₂), 53.3 (d, J_{CP} = 12 Hz, NCH₂P), 29.0 (s, CHMe₂), 19.1, 14.2 (2s, CHMe₂) ppm. ³¹P{¹H} NMR (161.95 MHz, CD₂Cl₂, 298 K) δ – 41.0 (s) ppm.

trans-[RuCl₂{(*R,R*)-^{*i*}Pr-pybox}(1-H-PTA)][Cl] (2c):

Yield: 0.069 g, 80%. Conductivity (acetone, 293 K): $\Lambda = 18 \text{ S cm}^2 \text{ mol}^{-1}$. S_{293 K} (H₂O): 22.45 mg/mL. ¹H NMR (400.13 MHz, CD₂Cl₂, 298 K) δ 7.98 (m, 1H, H⁴ C₅H₃N), 7.87 (m, 2H, H^{3,5} C₅H₃N), 4.99 (br, 5H, NCH₂N), 4.83 (m, 3H, OCH₂, NCH₂N), 4.70 (m, 2H, OCH₂), 4.60 (br, 6H, NCH₂P), 4.01 (m, 2H, CH^{*i*}Pr), 2.10 (m, 2H, CHMe₂), 1.08 (d, ³J_{HH} = 6.8 Hz, 6H, CHMe₂), 0.72 (d, ³J_{HH} = 6.0 Hz, 6H, CHMe₂) ppm. ¹³C{¹H} NMR (100.61 MHz, CD₂Cl₂, 298 K) δ 164.8 (s, OCN), 147.5 (s, C^{2,6} C₅H₃N), 134.7 (s, C⁴ C₅H₃N), 123.1 (s, C^{3,5} C₅H₃N), 72.2 (s, CH^{*i*}Pr), 72.1 (s, NCH₂N), 71.3 (s, OCH₂), 53.5 (s, NCH₂P), 29.2 (s, CHMe₂), 18.9, 14.1 (2s, CHMe₂) ppm. ³¹P{¹H} NMR (161.95 MHz, CD₂Cl₂, 298 K) δ – 24.9 (s) ppm.

trans-[RuCl₂{(*R,R*)-^{*i*}Pr-pybox}(1-CH₃-PTA)][I] (3c).

Yield: 0.080 g, 80%. Conductivity (acetone, 293 K): $\Lambda = 97 \text{ S cm}^2 \text{ mol}^{-1}$. S_{293 K} (H₂O): 7.10 mg/mL. ¹H NMR (300.13 MHz, CD₂Cl₂, 298 K) δ 7.99 (m, 1H, H⁴ C₅H₃N), 7.89 (m, 2H, H^{3,5} C₅H₃N), 5.69 (m, 2H, NCH₂N), 5.47 (m, 2H, NCH₂N), 4.96 (m, 2H,

NCH₂N), 4.85 (m, 2H, OCH₂), 4.74 (pt, 2H, ³J_{HH} = 9.4 Hz, ²J_{HH} = 9.4 Hz, OCH₂), 4.49 (m, 6H, NCH₂P), 4.21 (m, 2H, CHⁱPr), 3.29 (s, 3H, NCH₃), 2.06 (m, 2H, CHMe₂), 1.10 (d, ³J_{HH} = 7.2 Hz, 6H, CHMe₂), 0.71 (d, ³J_{HH} = 6.8 Hz, 6H, CHMe₂) ppm. ³¹P{¹H} NMR (161.95 MHz, CD₂Cl₂, 298 K) δ – 16.0 (s) ppm.

***trans*-[RuCl₂{(*R,R*)-ⁱPr-pybox}(1-CH₂=CHCH₂-PTA)][I] (4c):**

Yield: 0.078 g, 75%. Conductivity (acetone, 293 K): $\Lambda = 91 \text{ S cm}^2 \text{ mol}^{-1}$. S_{293 K} (H₂O): 9.20 mg/mL. ¹H-NMR (400.13 MHz, CD₂Cl₂, 298 K) δ 7.99 (m, 1H, H⁴ C₅H₃N), 7.90 (m, 2H, H^{3,5} C₅H₃N), 5.96 (m, 1H, CH₂=CHCH₂), 5.94–5.85 (m, 3H, CH₂=CHCH₂ and R-NCH₂N), 5.47 (m, 1H, R-NCH₂N), 5.20 (m, 1H, R-NCH₂N), 5.03 (m, 1H, NCH₂N), 4.93 (m, 1H, R-NCH₂P), 4.80–4.71 (m, 6H, OCH₂, R-NCH₂P), 4.55–4.35 (m, 7H, NCH₂N, NCH₂P, CH₂=CHCH₂), 4.13 (m, 2H, CHⁱPr), 2.05 (m, 2H, CHMe₂), 1.10 (d, 6H, ³J_{HH} = 6.4 Hz, CHMe₂), 0.72 (d, 6H, ³J_{HH} = 5.2 Hz, CHMe₂) ppm. ¹³C{¹H} NMR (100.61 MHz, CD₂Cl₂, 298 K) δ 164.8 (s, OCN), 147.4 (s, C^{2,6} C₅H₃N), 135.3 (s, C⁴ C₅H₃N), 130.5 (s, CH₂=CHCH₂), 123.3 (s, C^{3,5} C₅H₃N), 122.8 (CH₂=CHCH₂), 79.6, 79.2 (2s, R-NCH₂N), 73.3 (d, ³J_{CP} = 5 Hz, NCH₂N), 72.0 (s, CHⁱPr), 71.5 (s, OCH₂), 70.4 (s, NCH₂N), 63.4 (s, CH₂=CHCH₂), 55.5 (d, J_{CP} = 16 Hz, R-NCH₂P), 50.6 (d, J_{CP} = 16 Hz, NCH₂P), 50.4 (d, J_{CP} = 14 Hz, NCH₂P), 29.4 (s, CHMe₂), 19.0, 14.3 (2s, CHMe₂) ppm. ³¹P{¹H} NMR (161.95 MHz, CD₂Cl₂, 298 K) δ – 14.2 (s) ppm.

***trans*-[RuCl₂{(*R,R*)-ⁱPr-pybox}(1-CH≡CCH₂-PTA)][Br] (5c):**

Yield: 0.077 g, 79%. Conductivity (acetone, 293 K): $\Lambda = 73 \text{ S cm}^2 \text{ mol}^{-1}$. S_{293 K} (H₂O): 8.50 mg/mL. ¹H NMR (400.13 MHz, CD₂Cl₂, 298 K) δ 7.98 (m, 1H, H⁴ C₅H₃N), 7.90 (m, 2H, H^{3,5} C₅H₃N), 5.96 (m, 2H, R-NCH₂N), 5.71 (m, 1H, R-NCH₂N), 5.50 (m, 1H, R-NCH₂N), 5.26 (m, 1H, CH≡CCH₂), 4.97–4.30 (m, 14H, CH≡CCH₂, NCH₂N, NCH₂P, OCH₂, CH≡CCH₂), 4.22 (m, 2H, CHⁱPr), 2.08 (m, 2H, CHMe₂), 1.10 (d, ³J_{HH} = 6.8 Hz, 6H, CHMe₂), 0.72 (d, ³J_{HH} = 6.4 Hz, 6H, CHMe₂) ppm. ¹³C{¹H} NMR (100.61 MHz, CD₂Cl₂, 298 K) δ 164.7 (s, OCN), 147.4 (s, C^{2,6} C₅H₃N), 135.3 (s, C⁴ C₅H₃N), 123.4 (s,

C^{3,5} C₅H₃N), 81.9 (s, CH≡CCH₂), 79.7, 79.4 (2s, R-NCH₂N), 71.9 (s, CHⁱPr), 71.5 (s, OCH₂), 70.4 (s, NCH₂N), 70.1 (s, CH≡CCH₂), 55.7 (s, CH≡CCH₂), 51.2 (s, R-NCH₂P), 50.4 (d, *J*_{CP} = 16 Hz, NCH₂P), 50.2 (d, *J*_{CP} = 14 Hz, NCH₂P), 29.4 (s, CHMe₂), 19.0, 14.3 (s, CHMe₂) ppm. ³¹P{¹H} NMR (161.95 MHz, CD₂Cl₂, 298 K) δ – 13.7 (s) ppm.

***trans*-[RuCl₂{(*R,R*)-ⁱPr-pybox}(1-PhCH₂-PTA)][Br] (6c):**

Yield: 0.094 g, 90%. Reaction time: 1.5 h. Conductivity (acetone, 293 K): *A* = 68 S cm² mol⁻¹. S_{293 K} (H₂O): 11.49 mg/mL. ¹H NMR (300.13, CD₂Cl₂, 298 K) δ 7.97 (m, 1H, H⁴ C₅H₃N), 7.87 (m, 2H, H^{3,5} C₅H₃N), 7.70–7.38 (m, 5H, Ph), 6.24 (m, 2H, NCH₂N), 5.23 (m, 1H, NCH₂N), 5.02 (m, 3H, NCH₂N), 4.81 (m, 4H, OCH₂, NCH₂P), 4.71 (m, 3H, OCH₂, NCH₂P), 4.54 (m, 3H, CH₂Ph, NCH₂P), 4.36 (m, 1H, NCH₂P), 4.12 (m, 1H, NCH₂P), 3.97 (m, 2H, CHⁱPr), 1.87 (m, 2H, CHMe₂), 0.89 (d, 6H, ³*J*_{HH} = 7.2 Hz, CHMe₂), 0.64 (d, ³*J*_{HH} = 6.8 Hz, 6H, CHMe₂) ppm. ¹³C{¹H} NMR (100.61 MHz, CD₂Cl₂, 298 K) δ 164.8, (d, ⁴*J*_{CP} = 4.0 Hz, OCN), 147.4 (s, C^{2,6} C₅H₃N), 135.3 (s, C⁴ C₅H₃N), 133.2, 130.8, 129.5, 129.0, 128.7, 128.4 (6s, Ph), 125.4 (s, C^{*ipso*} Ph), 123.3 (s, C^{3,5} C₅H₃N), 79.5, 79.2 (2s, R-NCH₂N), 72.1 (s, CHⁱPr), 71.3 (s, OCH₂), 70.2 (s, NCH₂N), 65.1 (s, PhCH₂), 55.5 (d, *J*_{CP} = 5 Hz, R-NCH₂P), 50.8 (d, *J*_{CP} = 13 Hz, NCH₂P), 50.4 (d, *J*_{CP} = 14 Hz, NCH₂P), 29.3 (s, CHMe₂), 18.7, 14.3 (2s, CHMe₂) ppm. ³¹P{¹H} NMR (121.49 MHz, CD₂Cl₂, 298 K) δ – 14.2 (s) ppm.

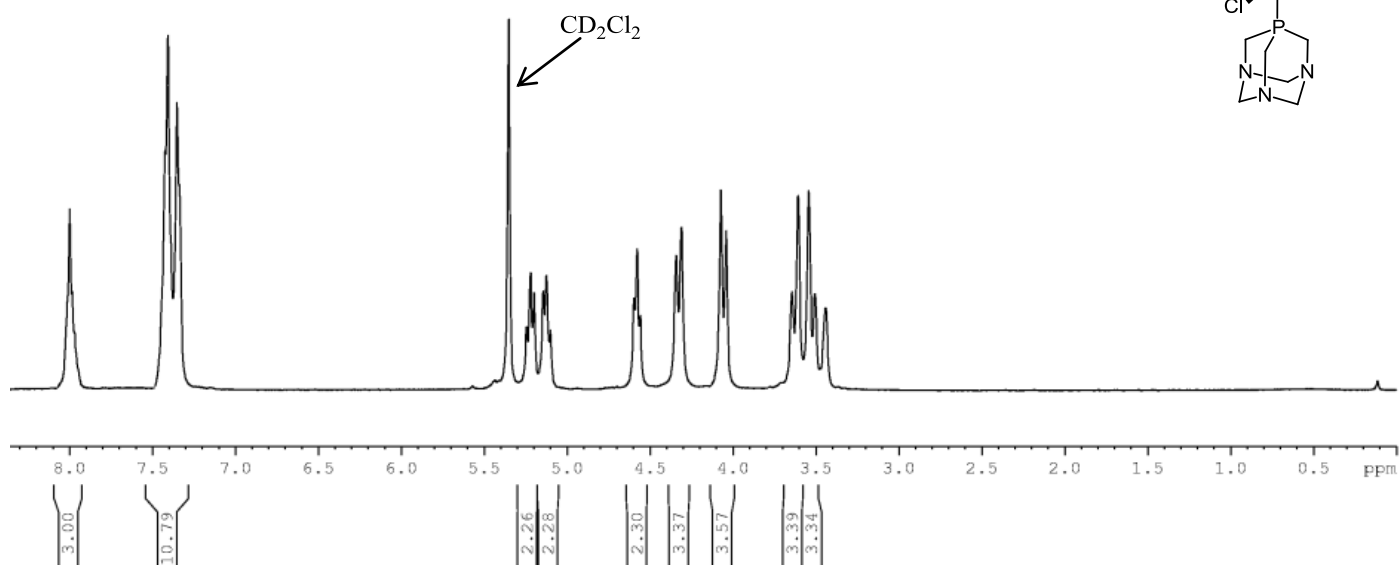
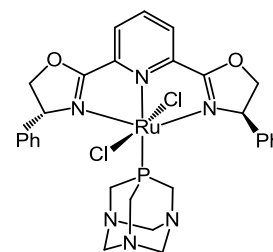
***trans*-[RuCl₂{(*R,R*)-ⁱPr-pybox}(1-PhCH₂-PTA)][Cl] (7c):**

Yield: 0.088 g, 90%. Reaction time: 2 h. Conductivity (acetone, 293 K): *A* = 70 S cm² mol⁻¹. S_{293 K} (H₂O): 8.59 mg/mL. ¹H NMR (300.13 MHz, CD₂Cl₂, 298 K) δ 7.99 (m, 1H, H⁴ C₅H₃N), 7.88 (m, 2H, H^{3,5} C₅H₃N), 7.71–7.38 (3m, 5H, Ph), 6.26 (m, 2H, R-NCH₂N), 5.15 (m, 1H, R-NCH₂N), 5.01 (m, 3H, R-NCH₂N), 4.81 (m, 4H, OCH₂, NCH₂P), 4.71 (m, 3H, OCH₂, NCH₂P), 4.55 (m, 3H, CH₂Ph, NCH₂P), 4.36 (m, 1H, NCH₂P), 4.14 (m, 1H, NCH₂P), 3.98 (m, 2H, CHⁱPr), 1.87 (m, 2H, CHMe₂), 0.89 (d, ³*J*_{HH} = 7.2 Hz, 6H, CHMe₂), 0.65 (d, ³*J*_{HH} = 6.8 Hz, 6H, CHMe₂) ppm. ¹³C{¹H} NMR

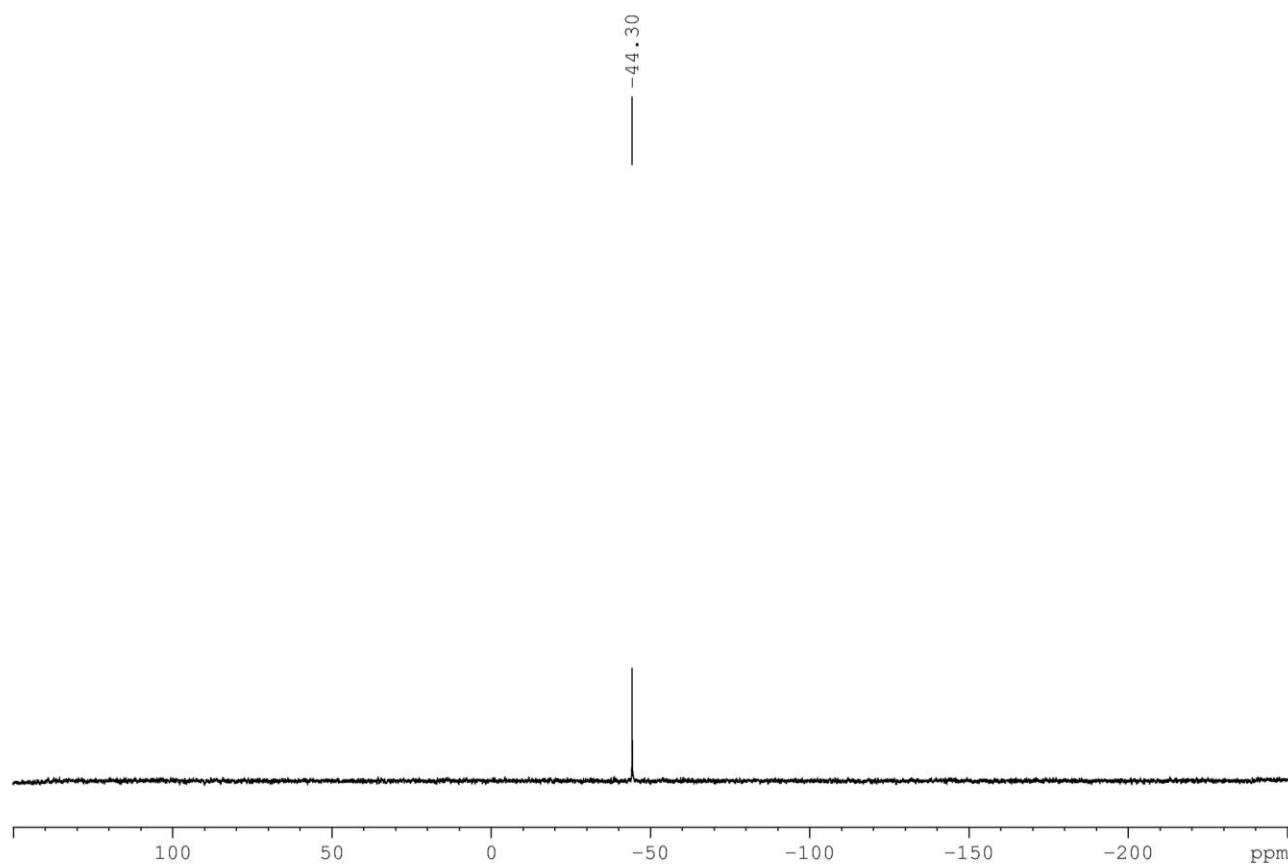
(100.61 MHz, CD₂Cl₂, 298 K) δ 164.8 (d, $^4J_{CP} = 4.0$ Hz, OCN), 147.4 (s, C^{2,6} C₅H₃N), 135.3 (s, C⁴ C₅H₃N), 133.2, 130.8, 129.5, 129.0, 128.7, 128.4 (6s, Ph), 125.4 (s, C^{*ipso*} Ph), 123.3 (br, C^{3,5} C₅H₃N), 79.5, 79.2 (2s, R-NCH₂N), 72.1 (s, CH^{*i*}Pr), 71.3 (s, OCH₂), 70.2 (s, NCH₂N), 65.1 (s, PhCH₂), 55.5 (d, $J_{CP} = 5$ Hz, R-NCH₂P), 50.8 (d, $J_{CP} = 13$ Hz, NCH₂P), 50.4 (d, $J_{CP} = 14$ Hz, NCH₂P), 29.3 (s, CHMe₂), 18.7, 14.3 (2s, CHMe₂) ppm.

³¹P{¹H} NMR (121.49 MHz, CD₂Cl₂, 298 K) δ - 14.3 (s) ppm.

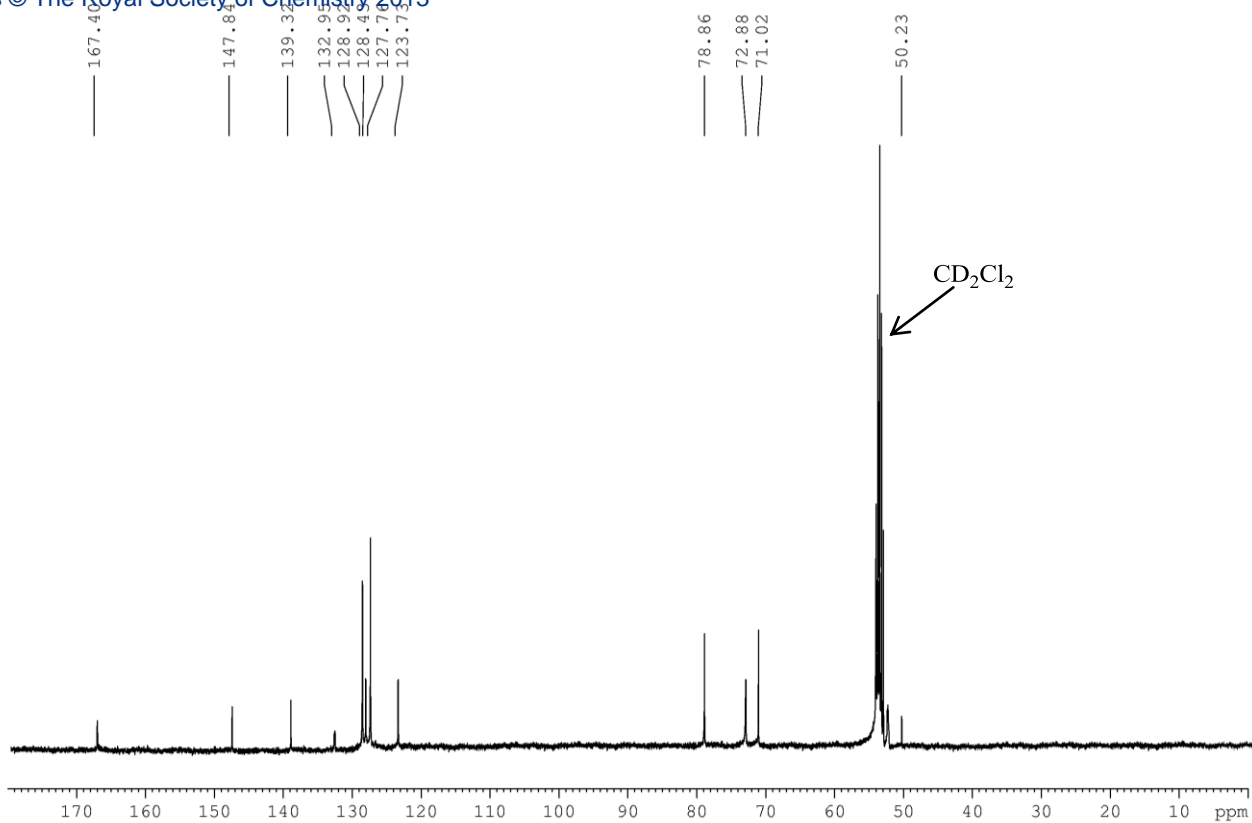
Selected NMR spectra:



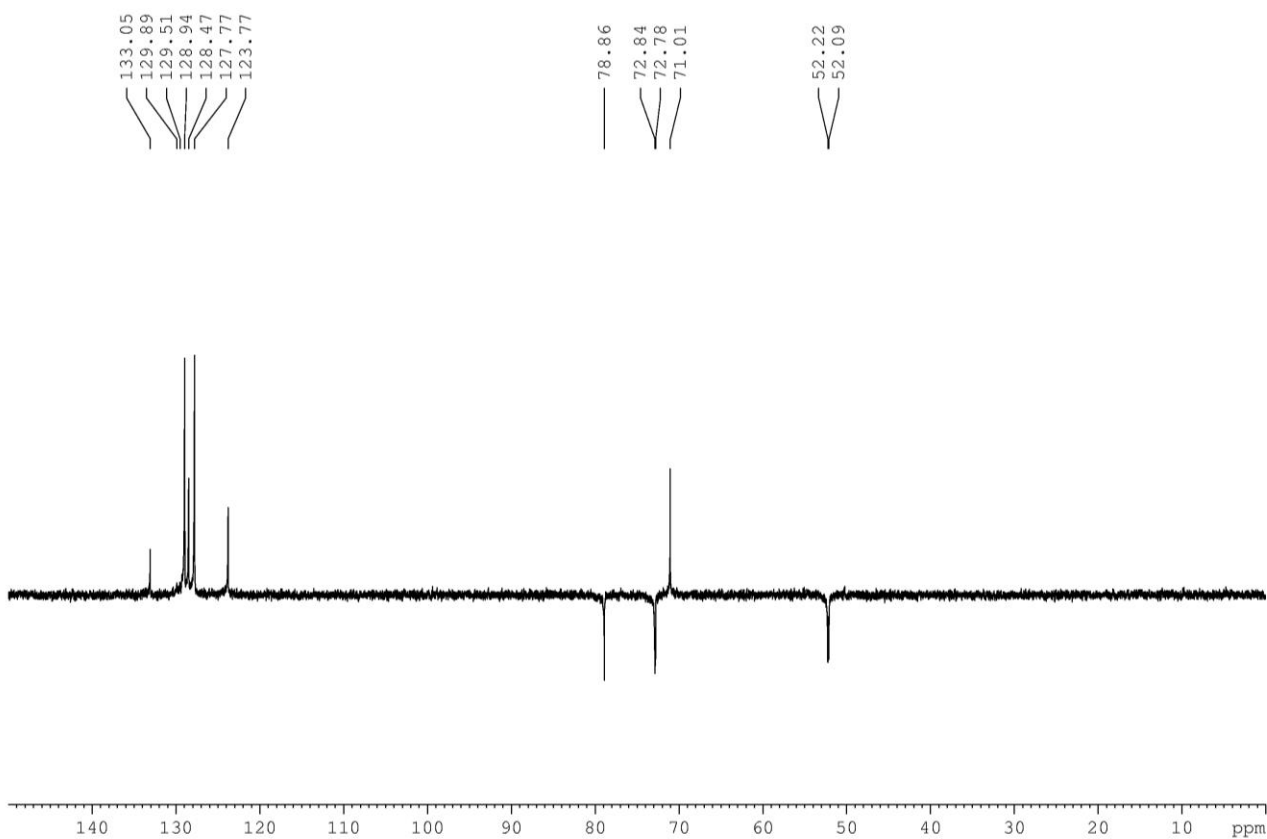
^1H NMR spectrum (CD_2Cl_2 , 298 K, NAV400) of complex **1a**



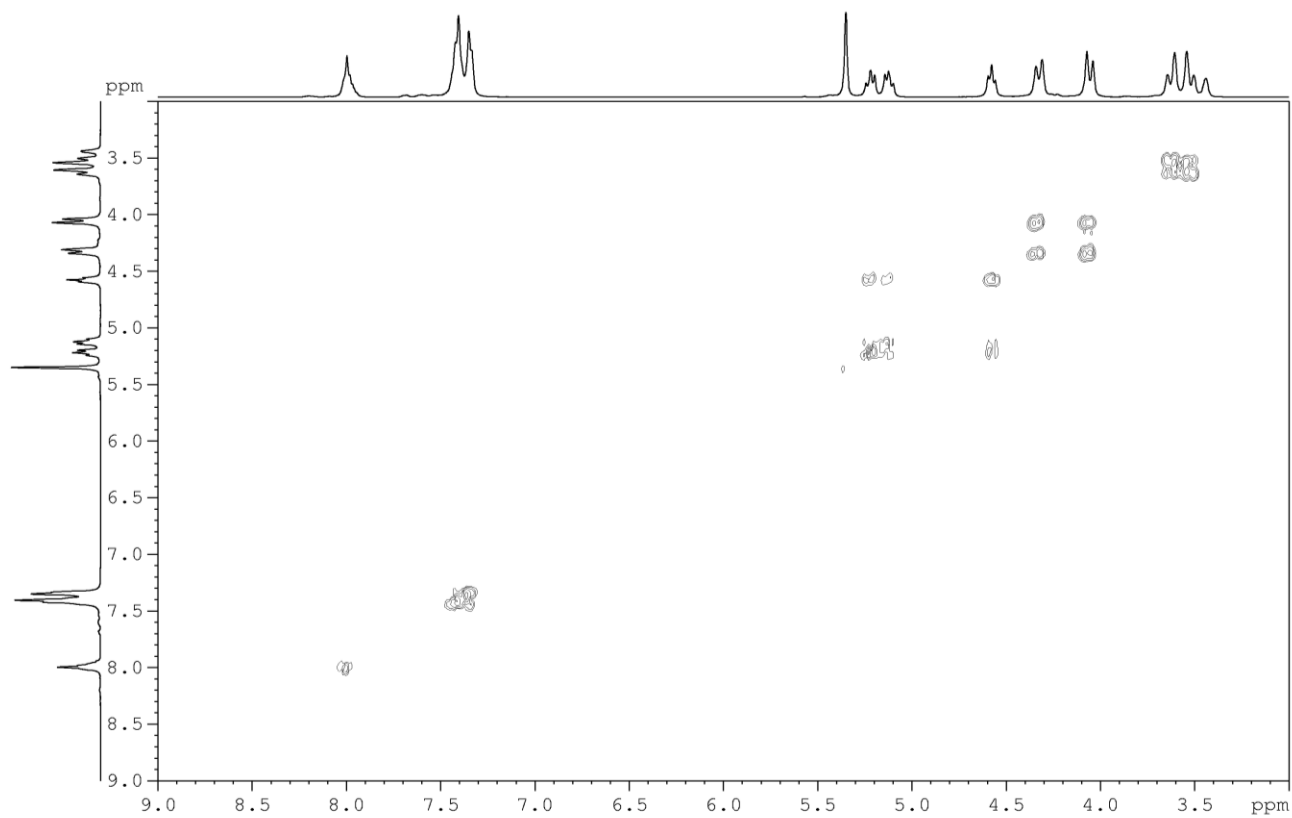
^{31}P NMR spectrum (CD_2Cl_2 , 298 K, NAV400) of complex **1a**



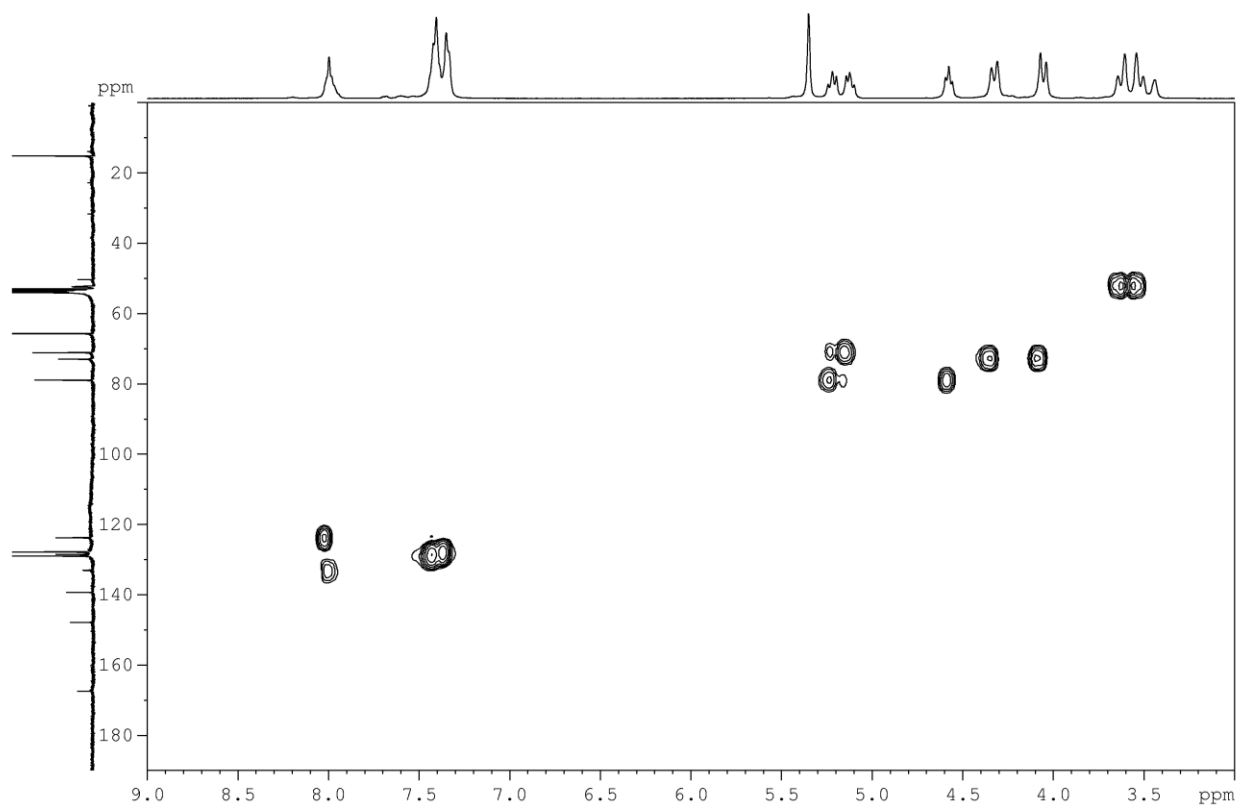
¹³C NMR spectrum (CD₂Cl₂, 298 K, NAV400) of complex **1a**



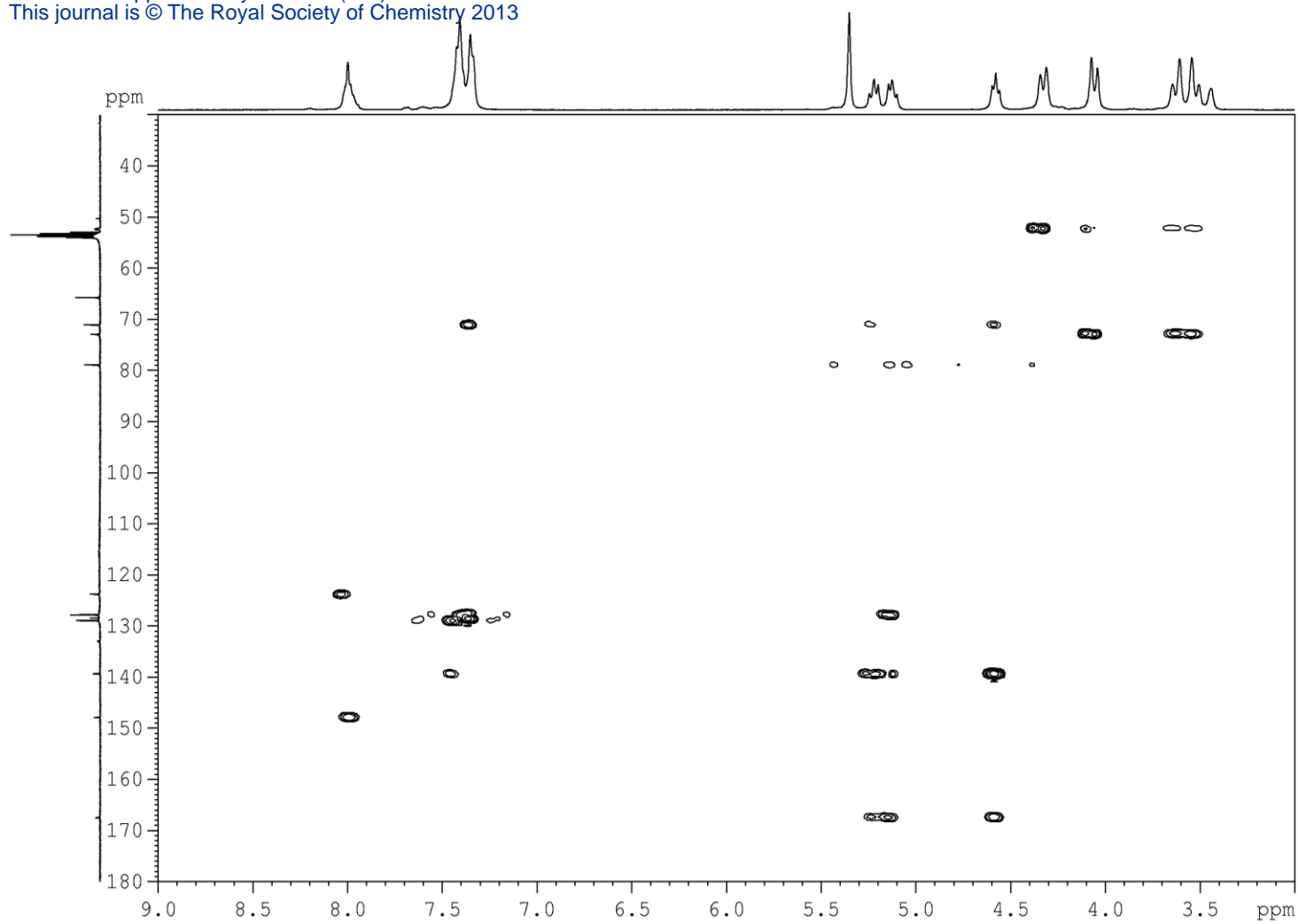
DEPT-135 NMR spectrum (CD₂Cl₂, 298 K, NAV400) of complex **1a**



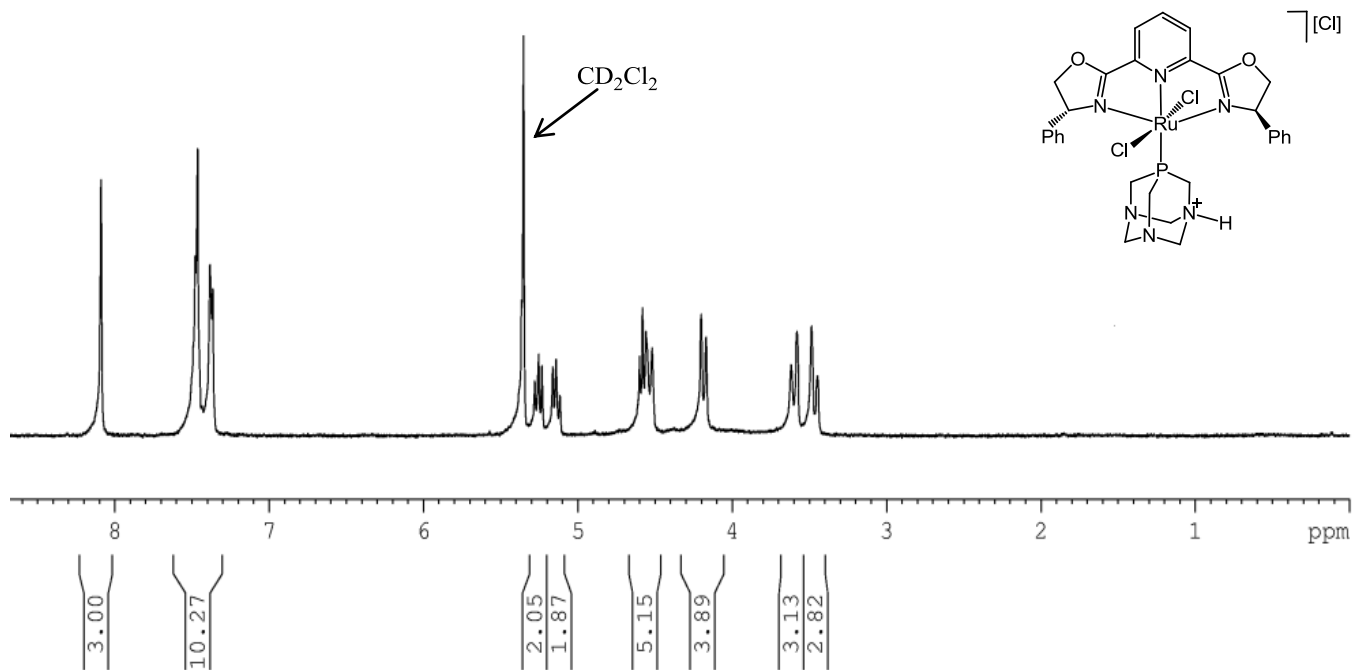
COSY HH NMR spectrum (CD₂Cl₂, 298 K, AV400) of complex **1a**



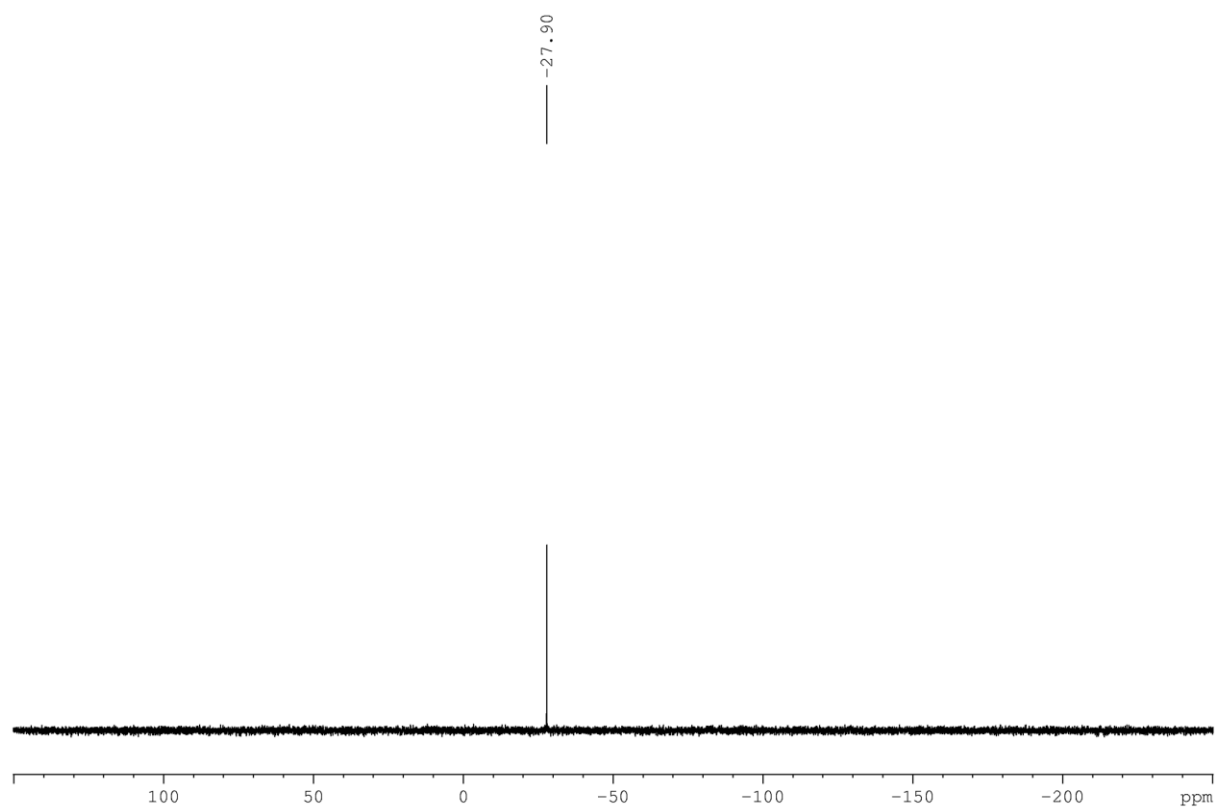
HSQC NMR spectrum (CD₂Cl₂, 298 K, AV400) of complex **1a**



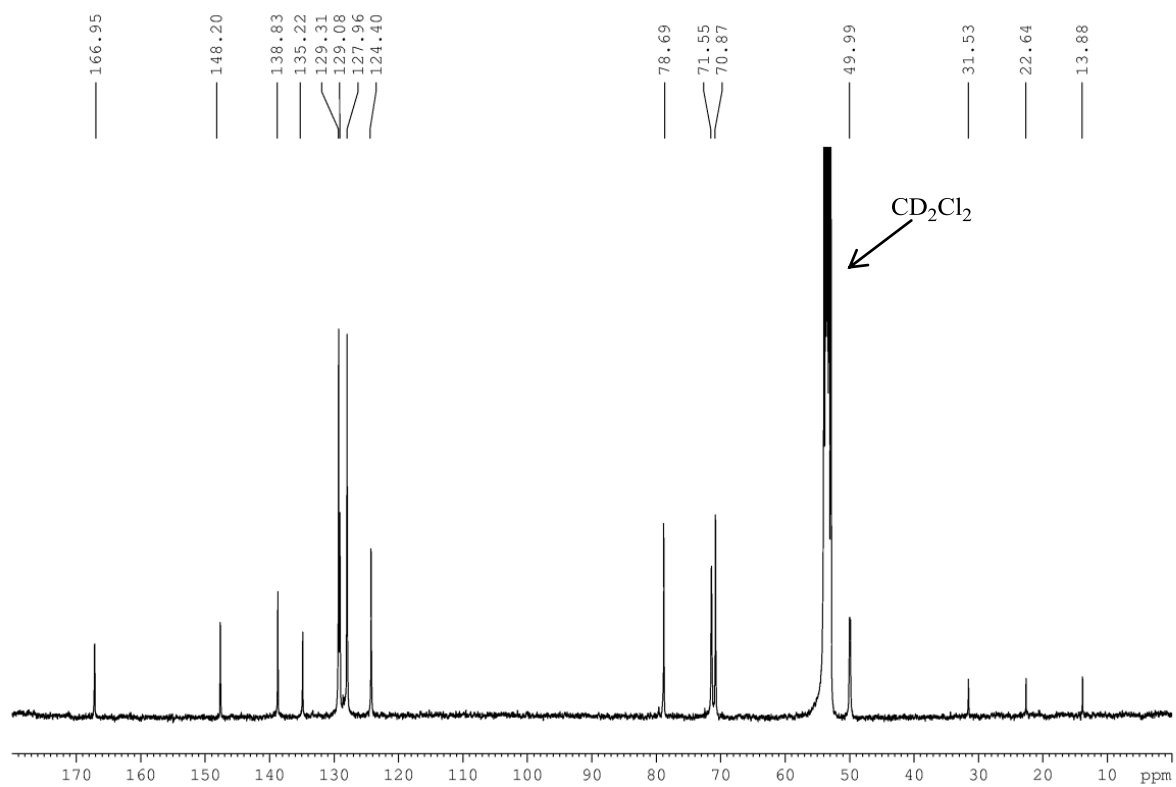
HMBC NMR spectrum (CD_2Cl_2 , 298 K, AV400) of complex **1a**



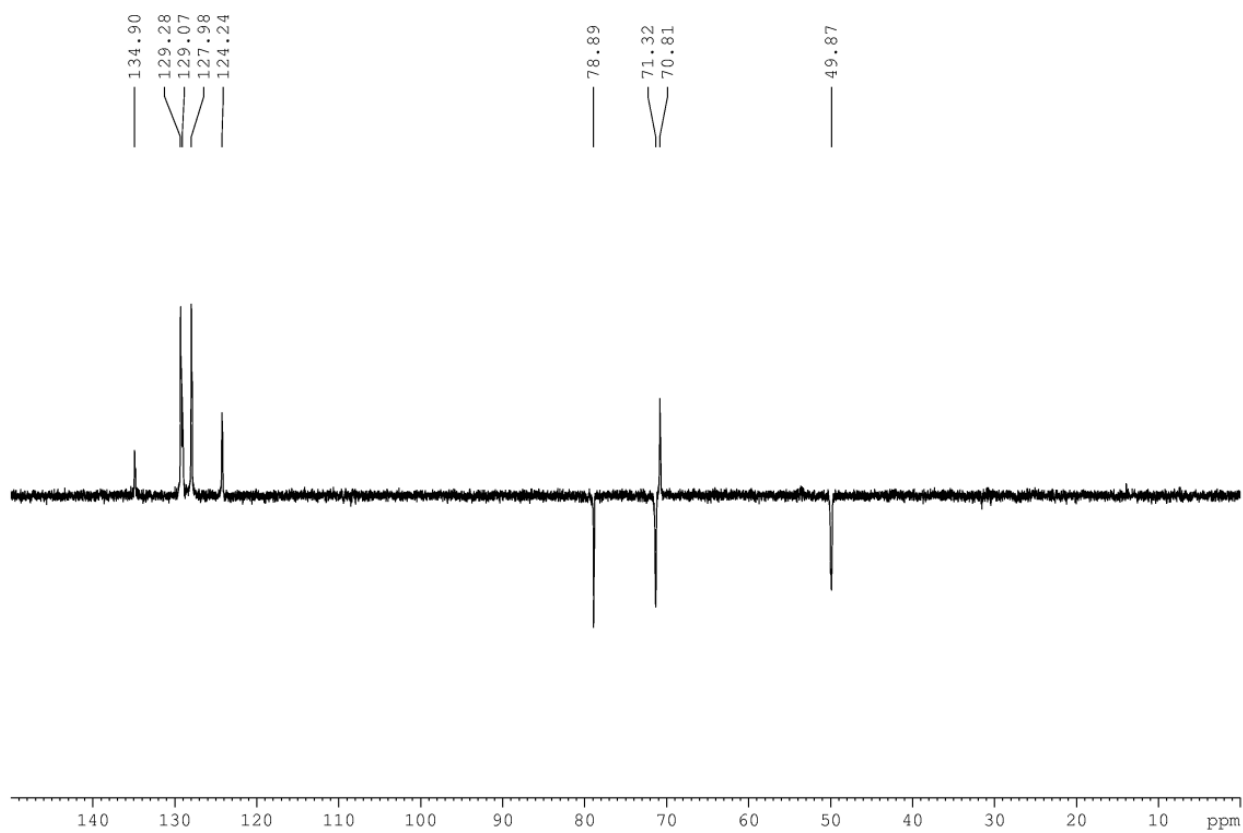
^1H NMR spectrum (CD_2Cl_2 , 298 K, NAV400) of complex **2a**



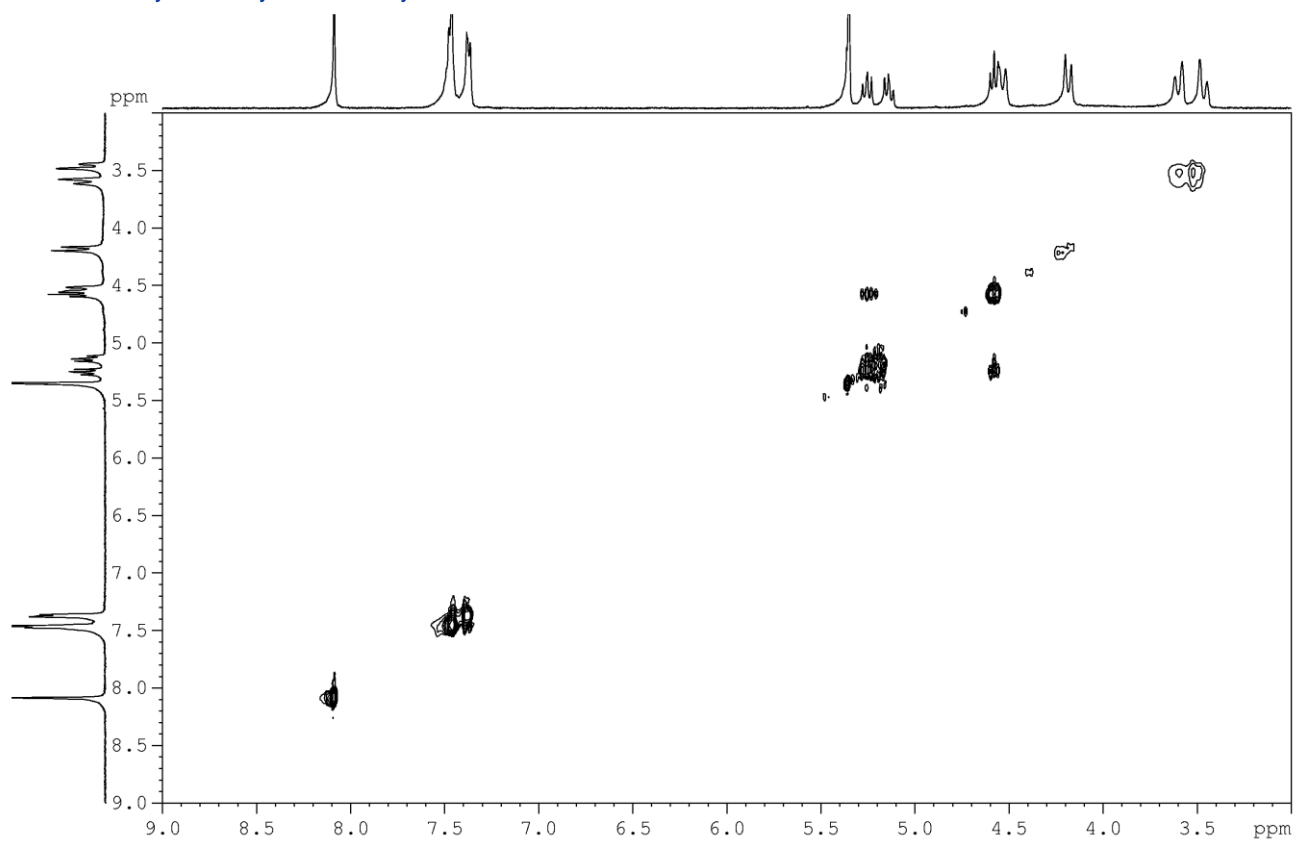
^{31}P NMR spectrum (CD_2Cl_2 , 298 K, NAV400) of complex **2a**



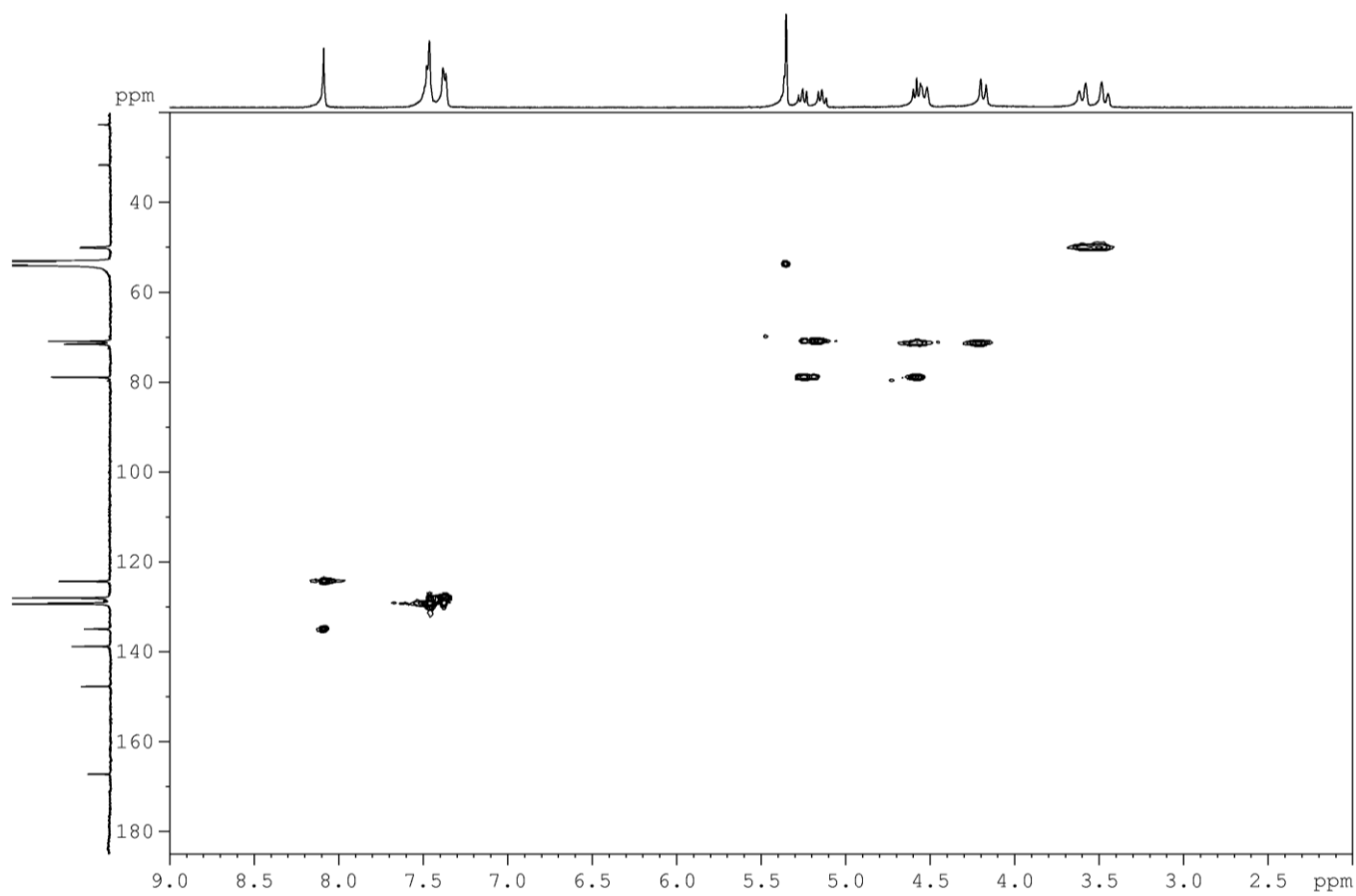
¹³C NMR spectrum (CD₂Cl₂, 298 K, AV400) of complex **2a**



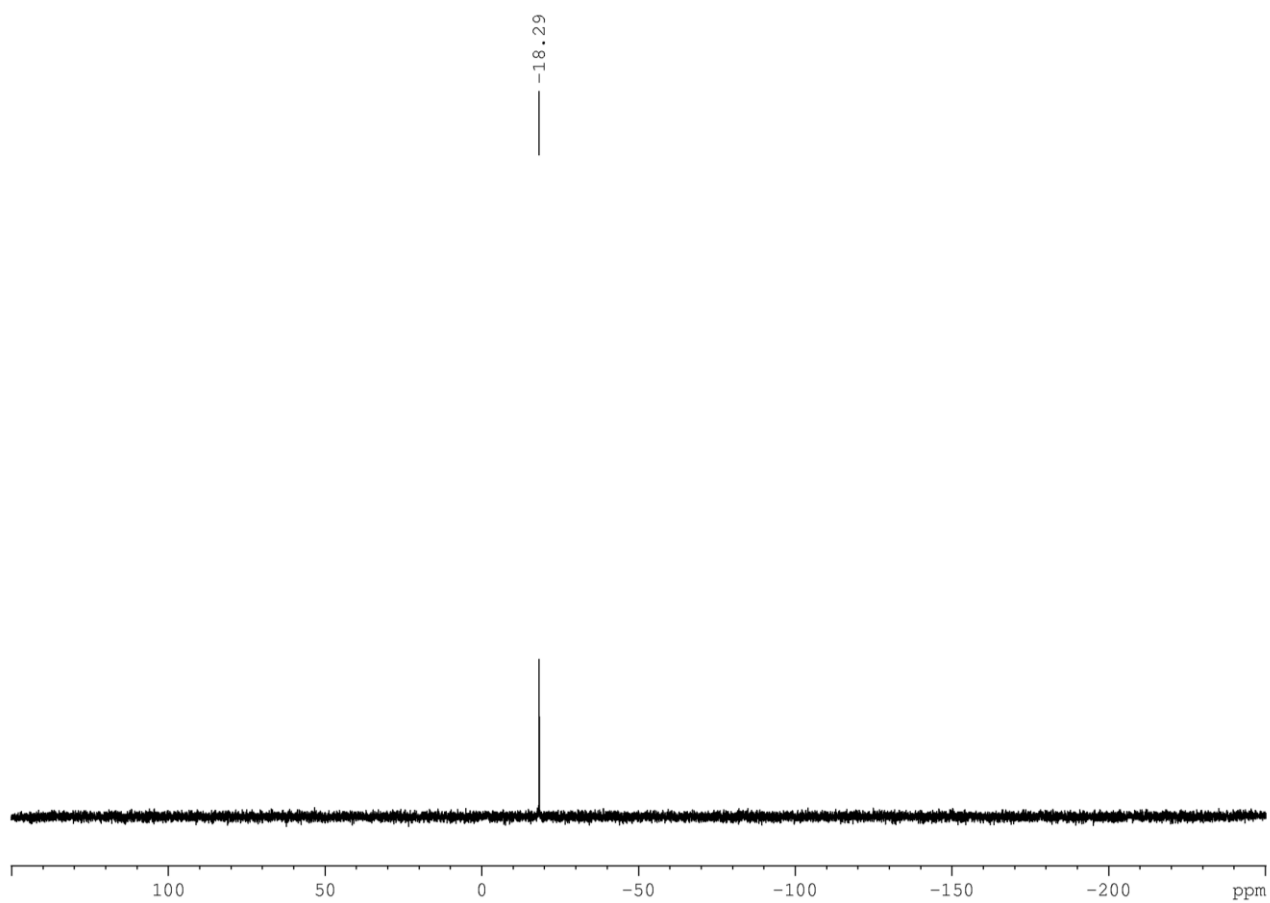
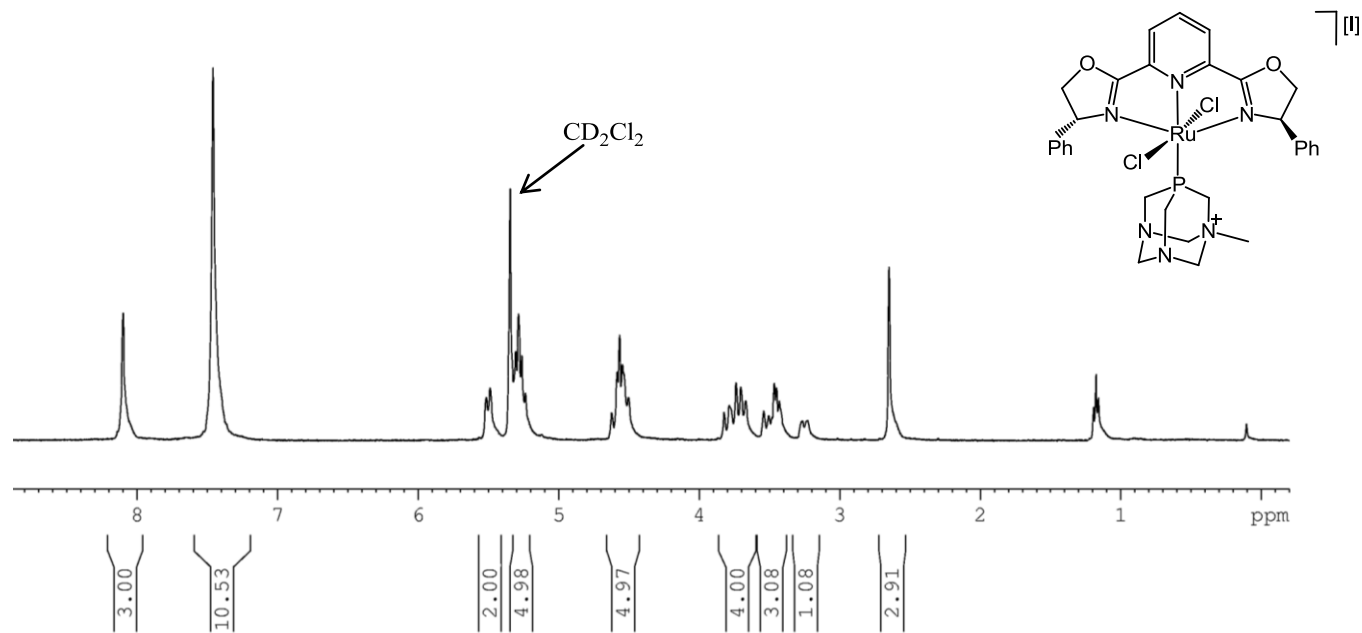
DEPT135- NMR spectrum (CD₂Cl₂, 298 K, NAV400) of complex **2a**

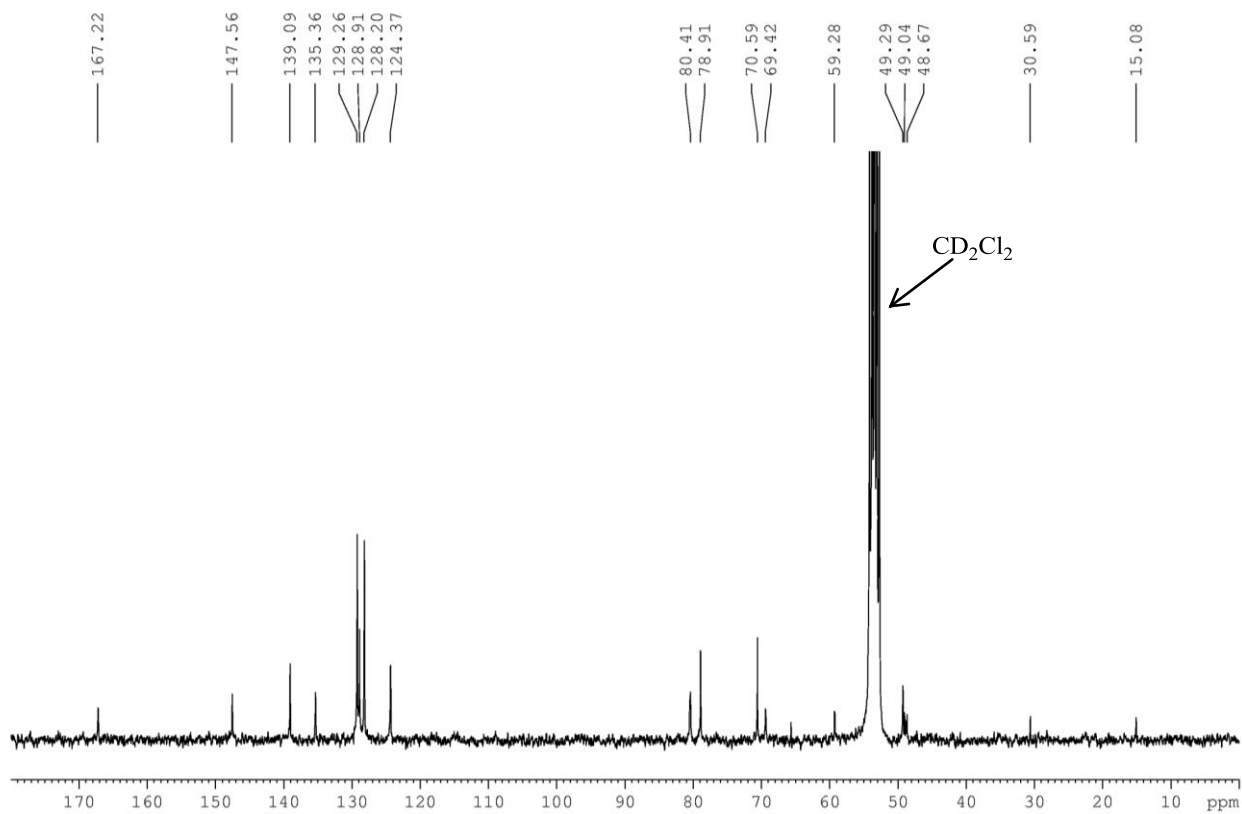


COSY HH NMR spectrum (CD₂Cl₂, 298 K, AV400) of complex **2a**

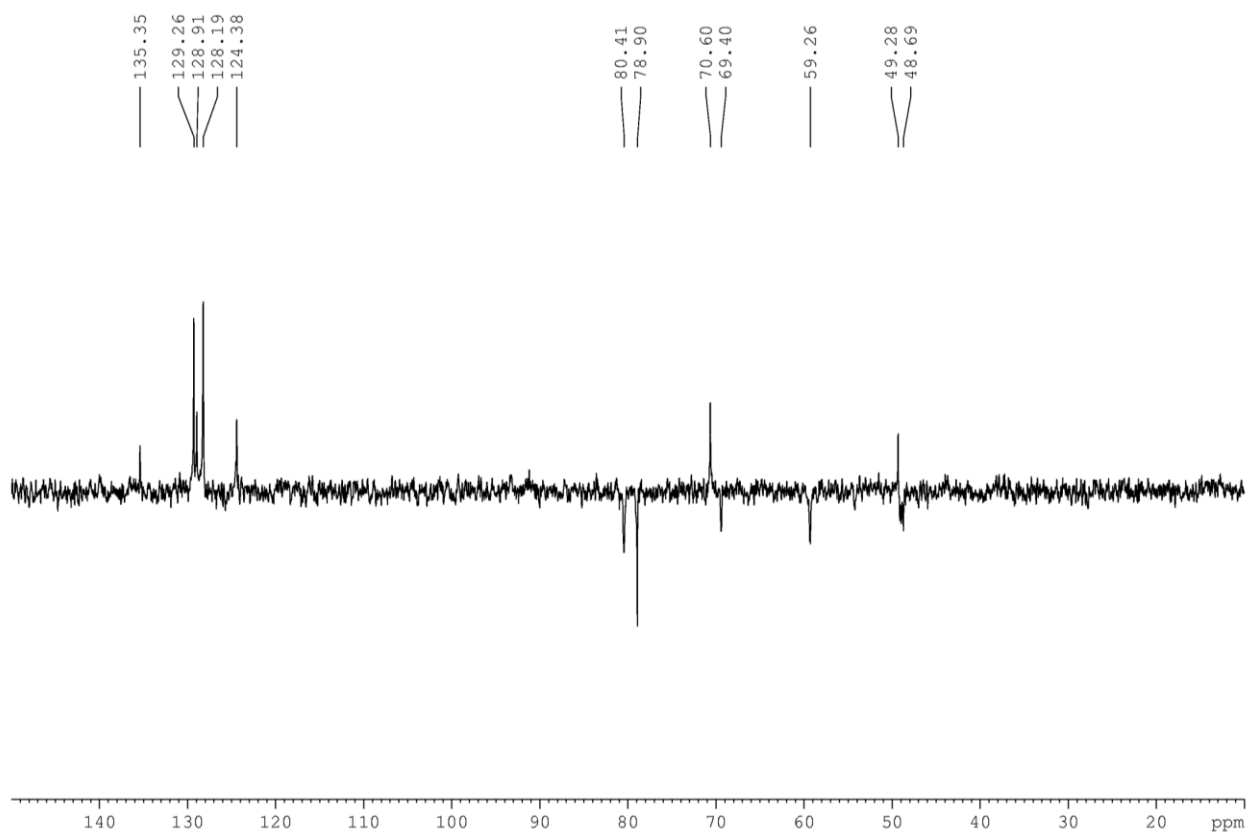


HSQC NMR spectrum (CD₂Cl₂, 298 K, AV400) of complex **2a**

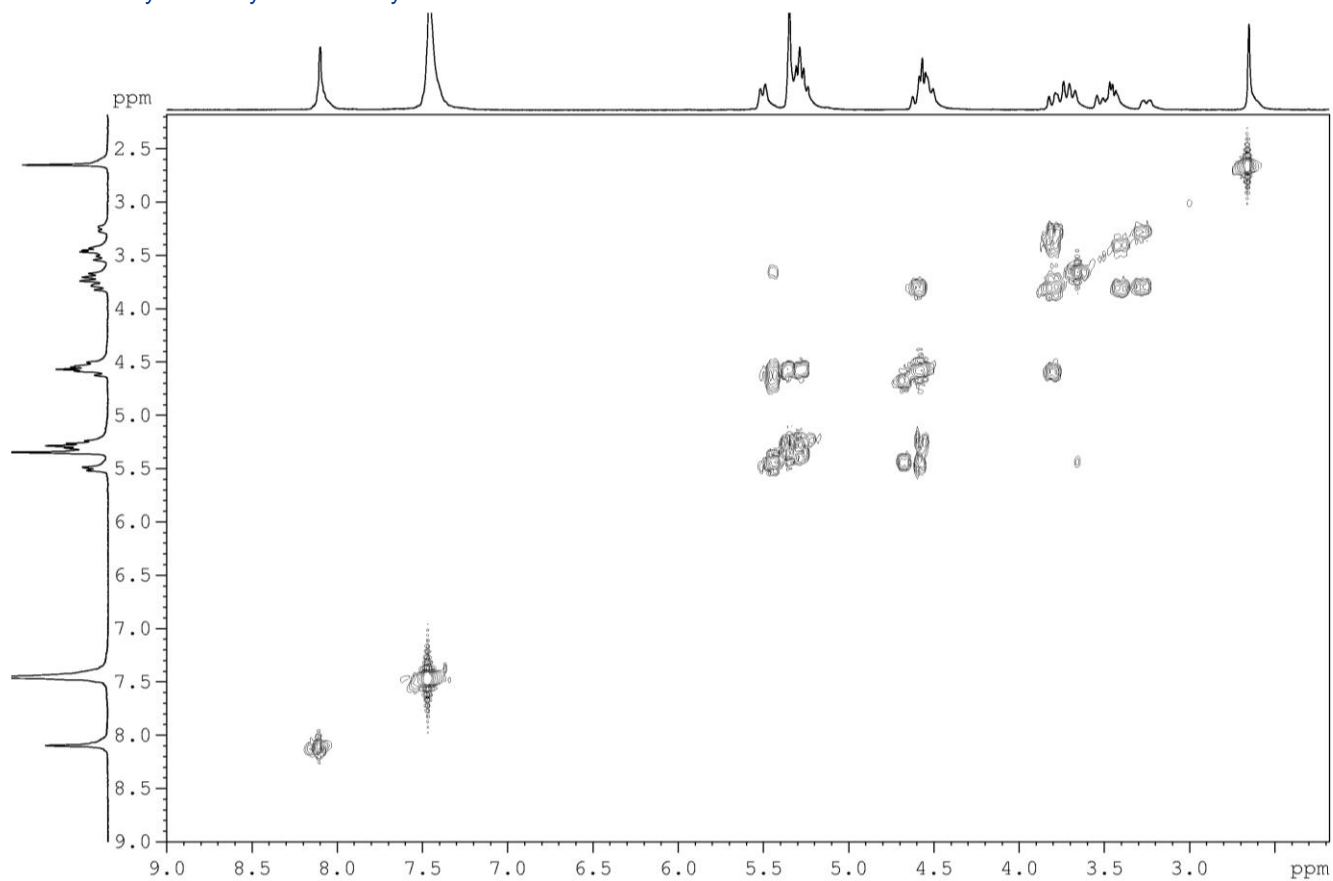




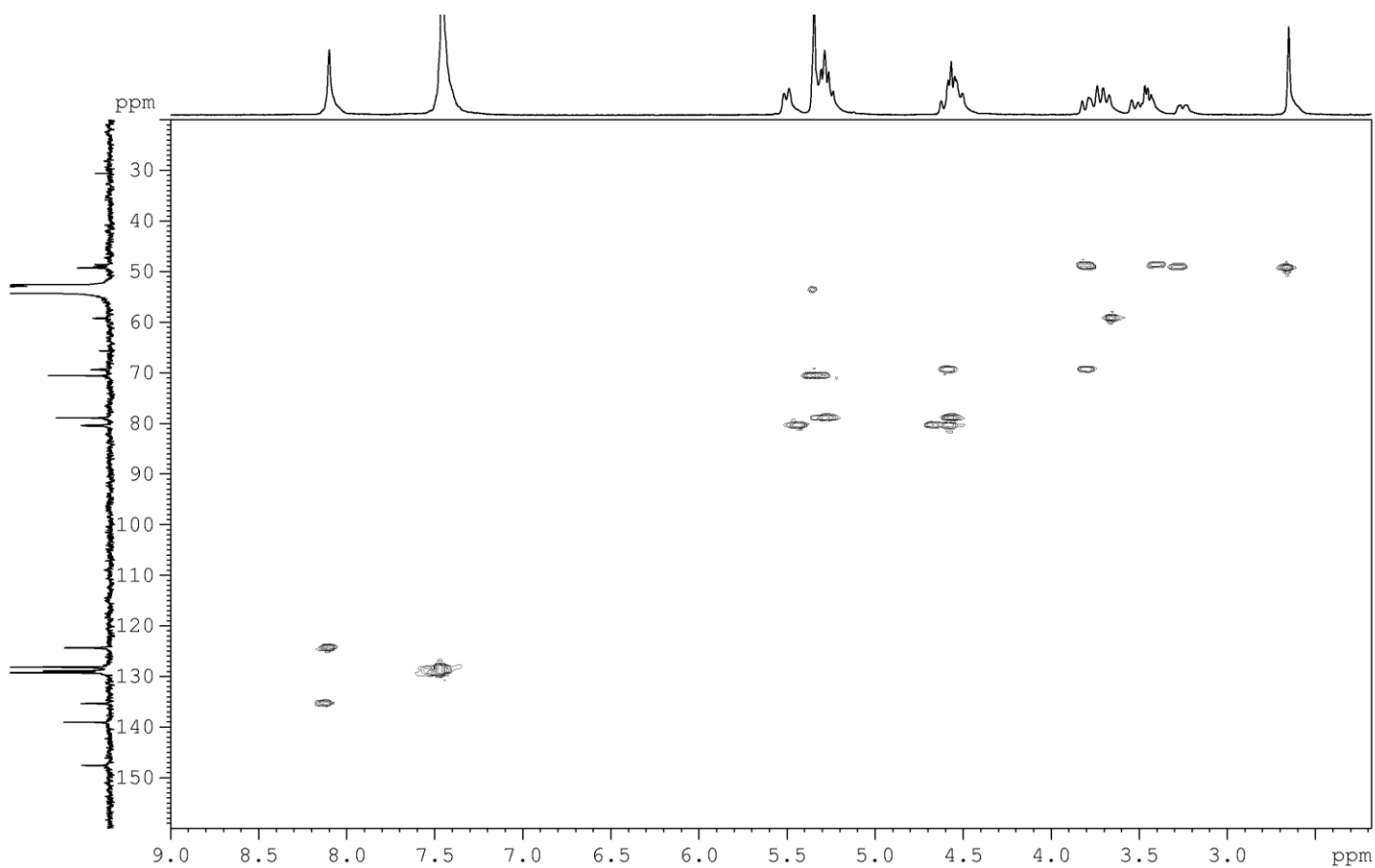
¹³C NMR spectrum (CD₂Cl₂, 298 K, AV300) of complex **3a**



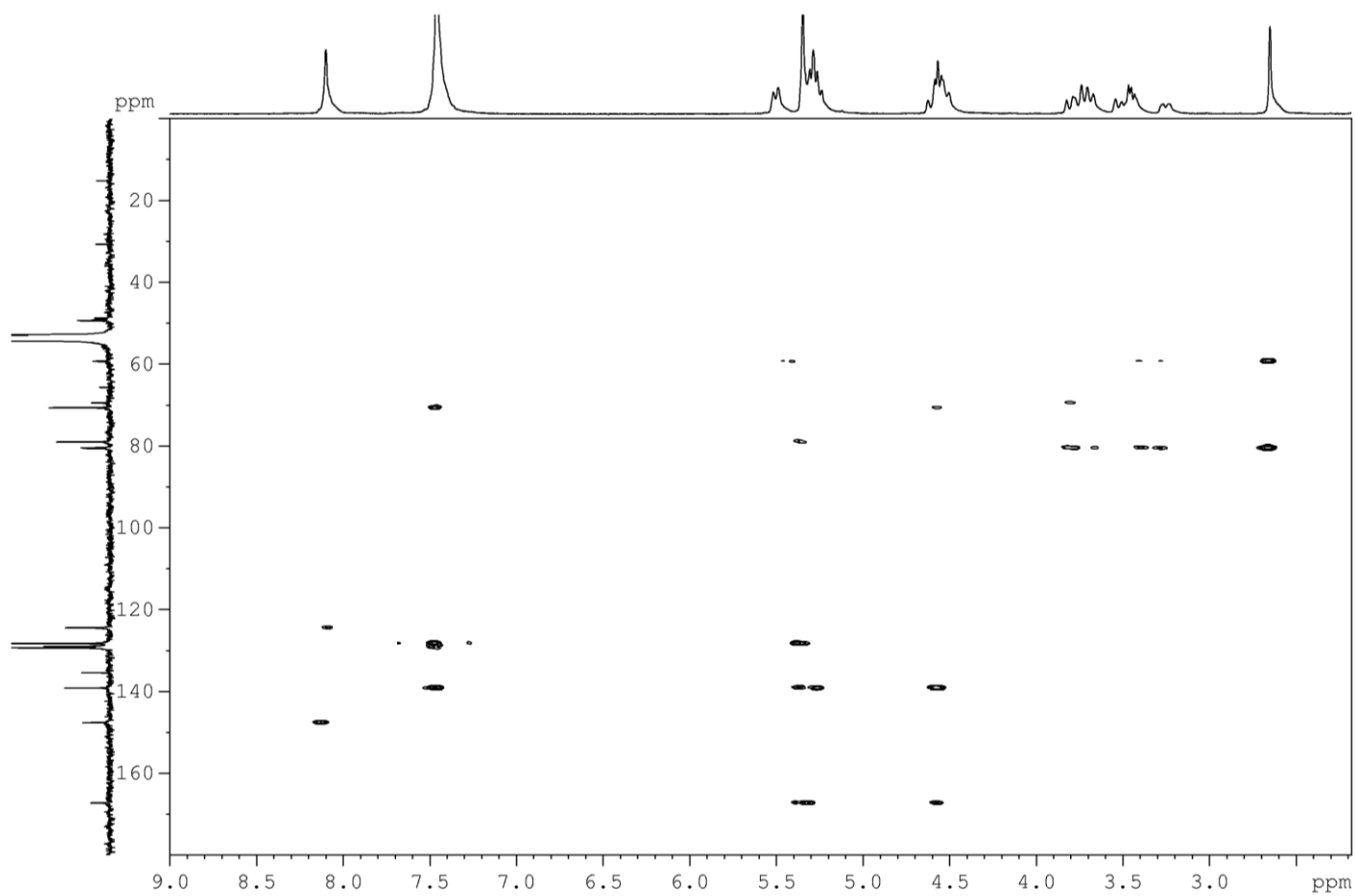
DEPT-135 NMR spectrum (CD₂Cl₂, 298 K, AV300) of complex **3a**



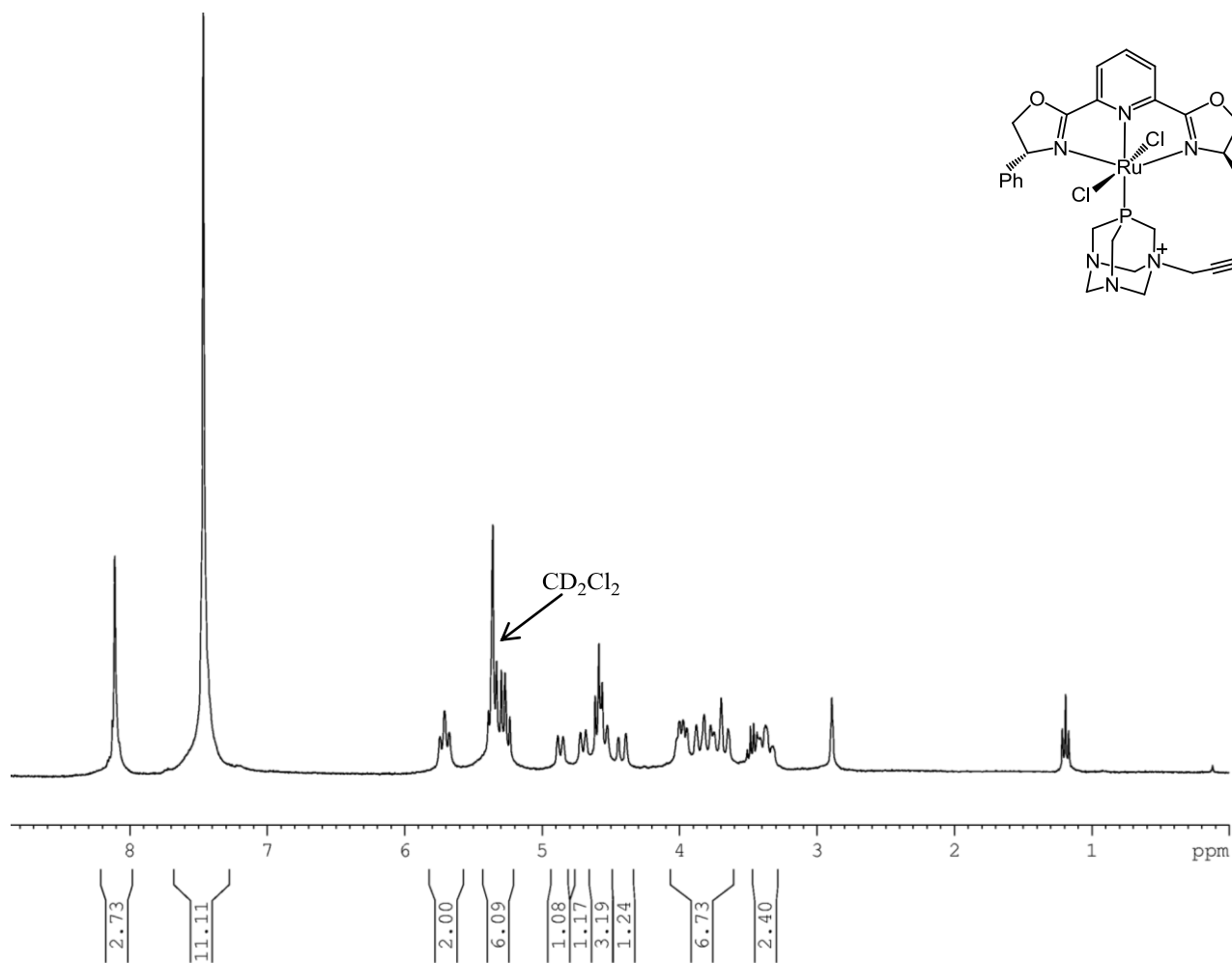
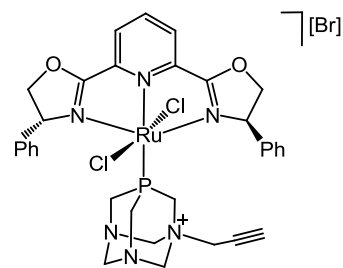
COSY HH NMR spectrum (CD₂Cl₂, 298 K, AV400) of complex **3a**



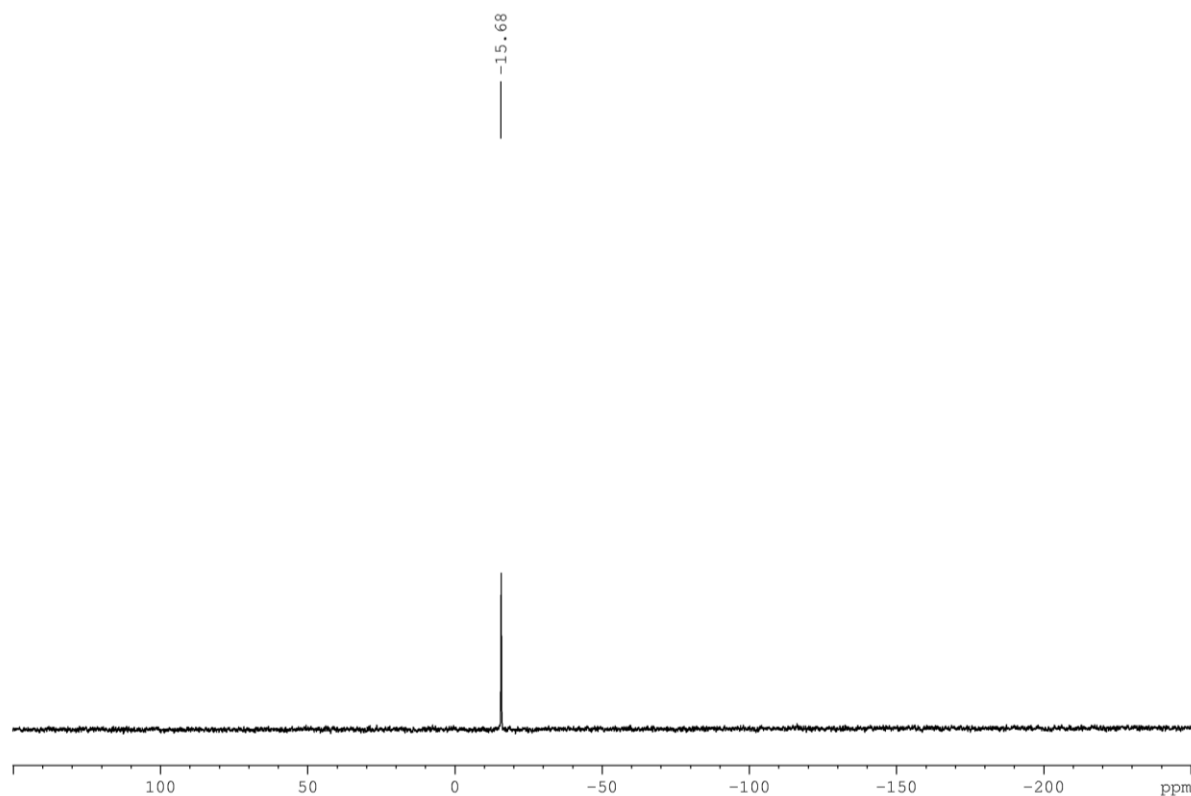
HSQC NMR spectrum (CD₂Cl₂, 298 K, AV400) of complex **3a**



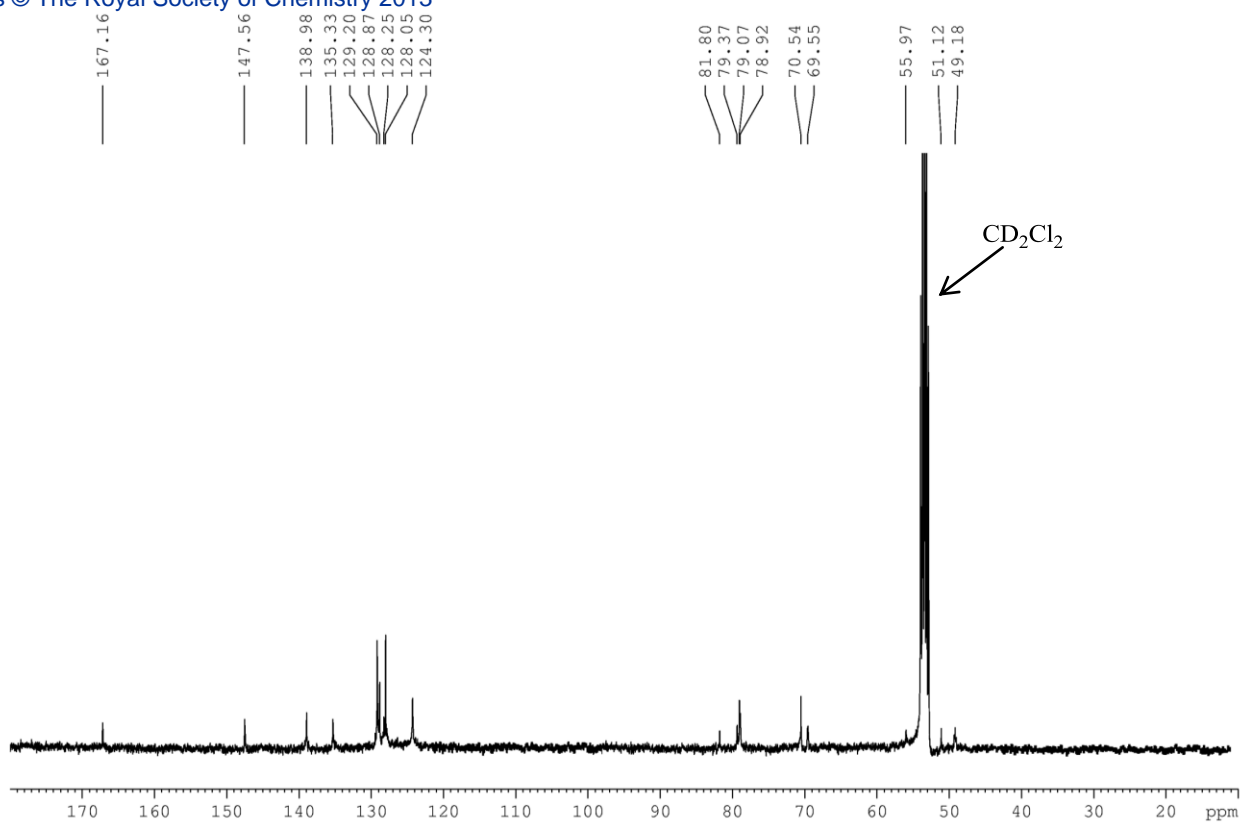
HMBC NMR spectrum (CD_2Cl_2 , 298 K, AV400) of complex **3a**



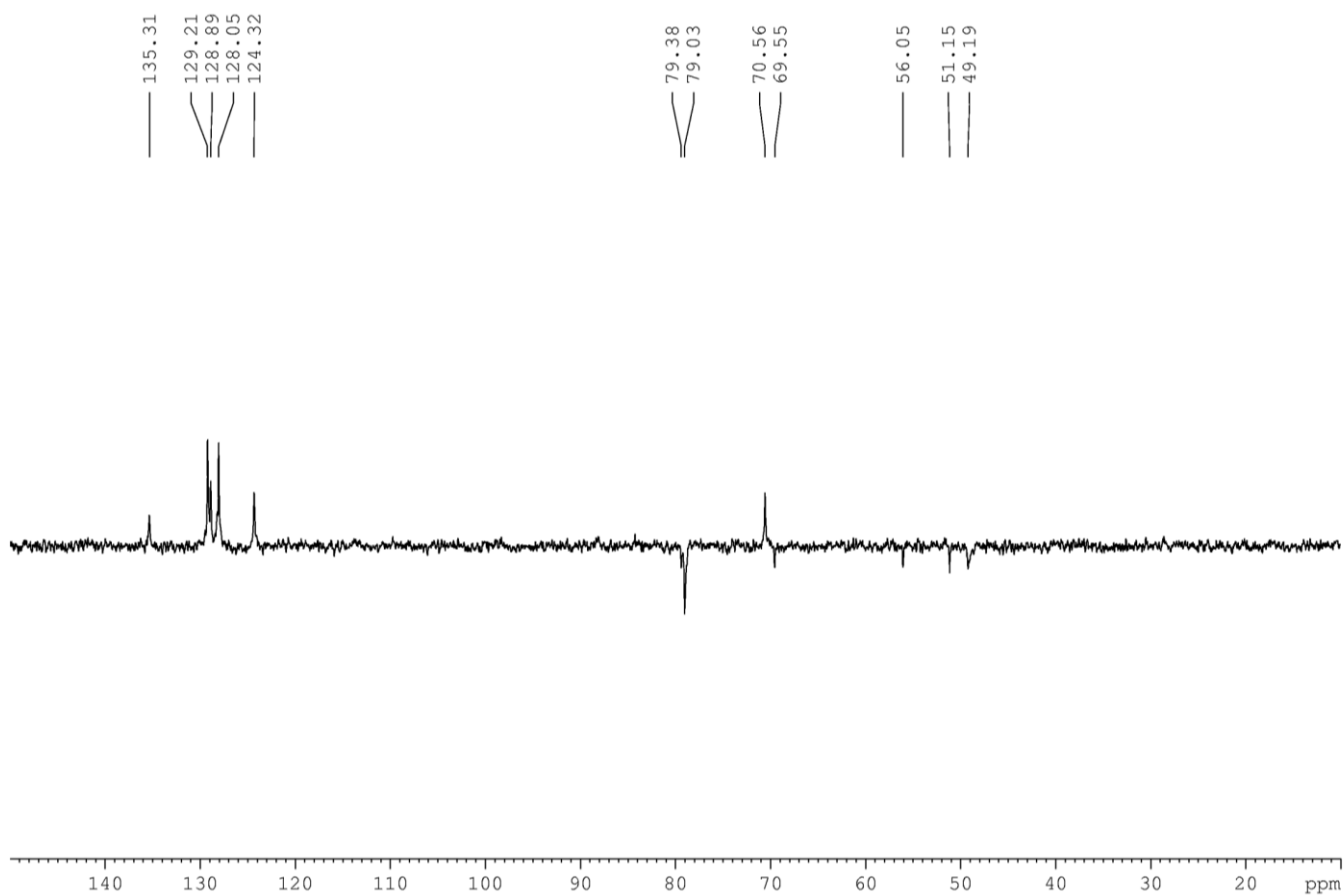
¹H NMR spectrum (CD₂Cl₂, 298 K, AV300) of complex **5a**



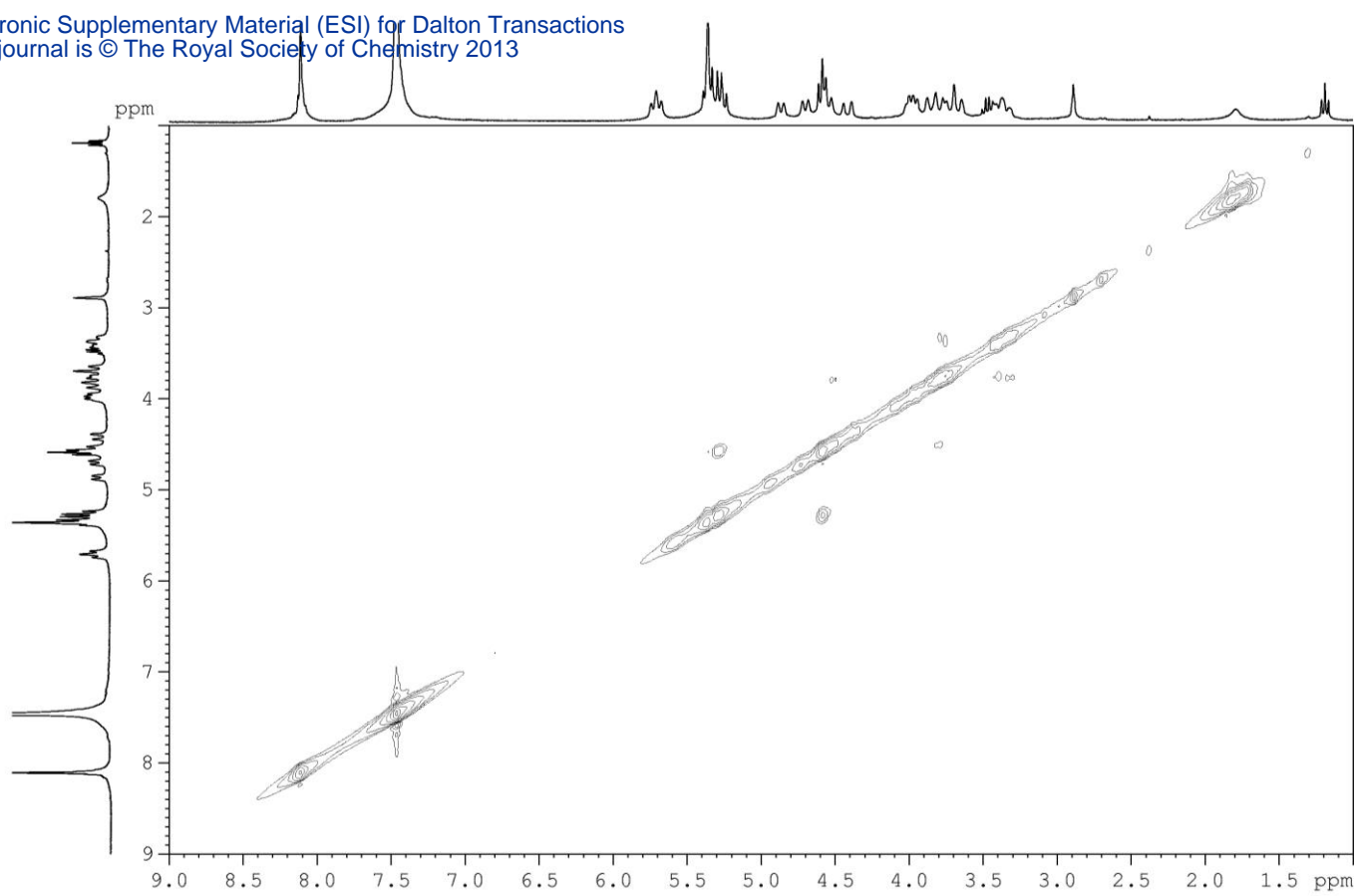
³¹P NMR spectrum (CD₂Cl₂, 298 K, AV300) of complex **5a**



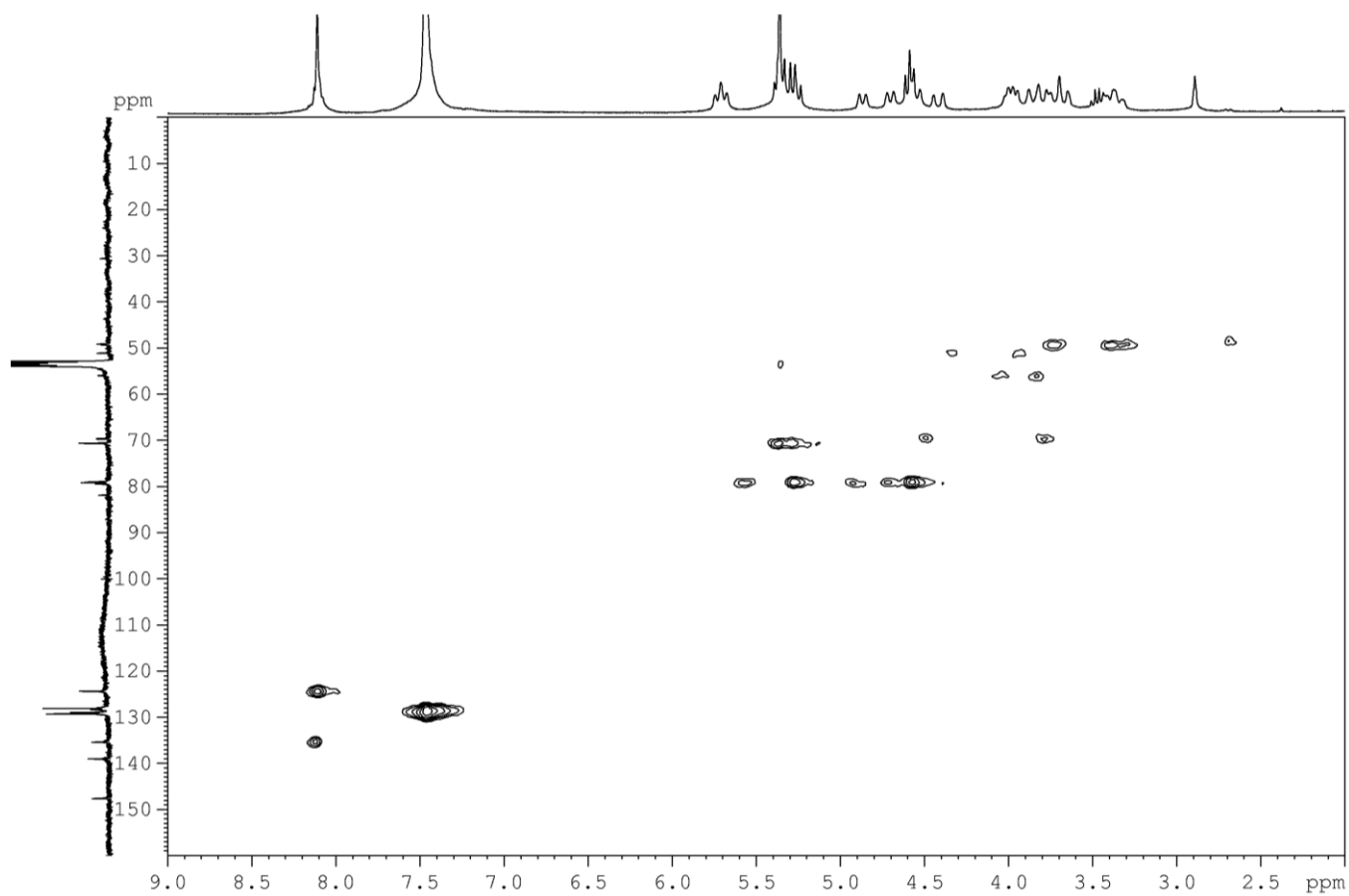
¹³C NMR spectrum (CD₂Cl₂, 298 K, NAV400) of complex **5a**



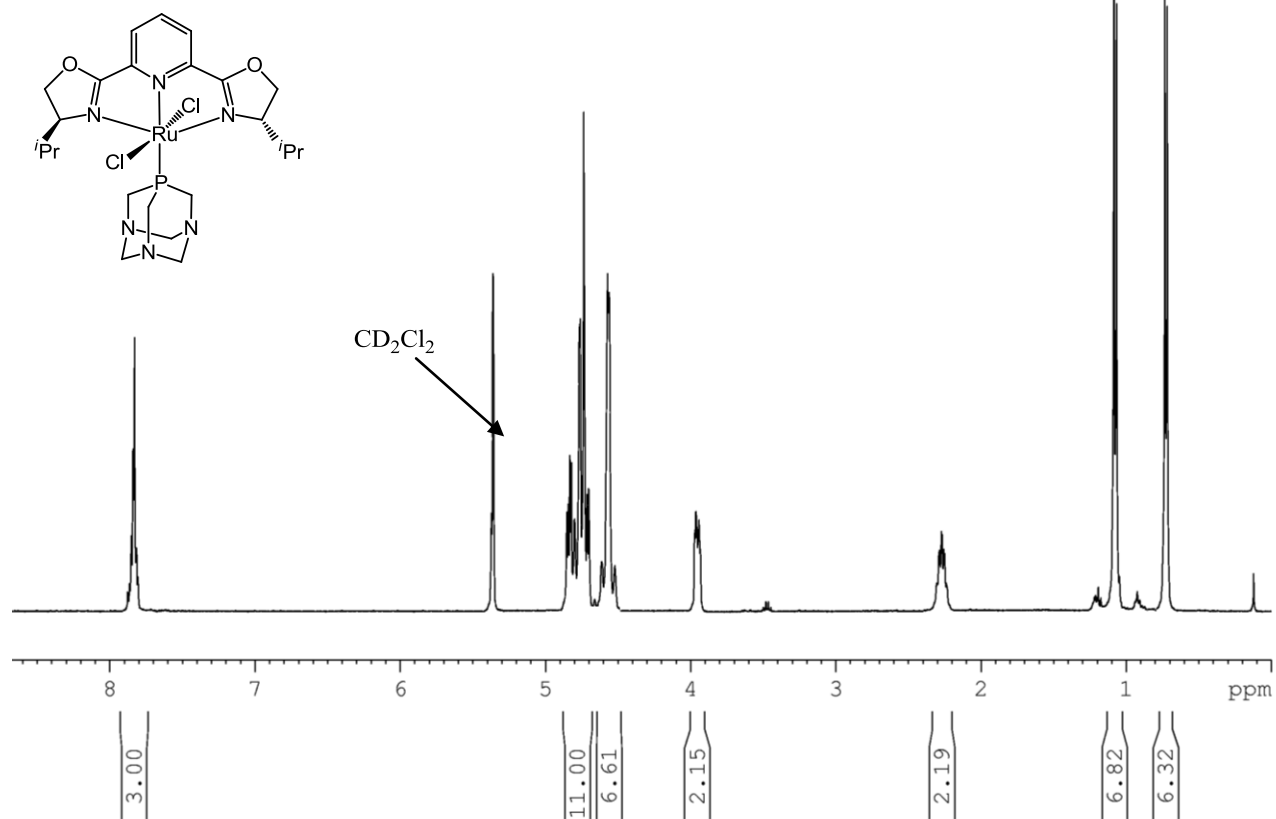
DEPT-135 NMR spectrum (CD₂Cl₂, 298 K, NAV400) of complex **5a**



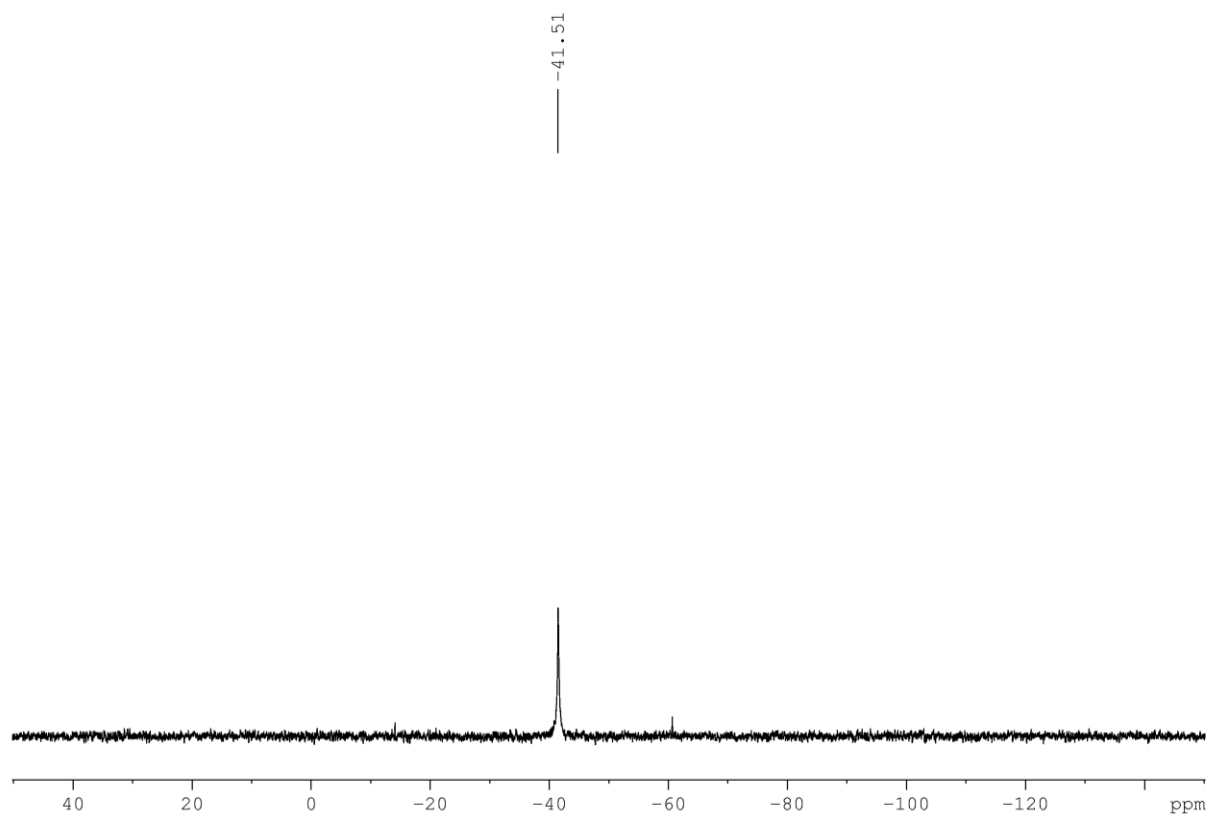
COSY HH NMR spectrum (CD_2Cl_2 , 298 K, AV400) of complex **5a**



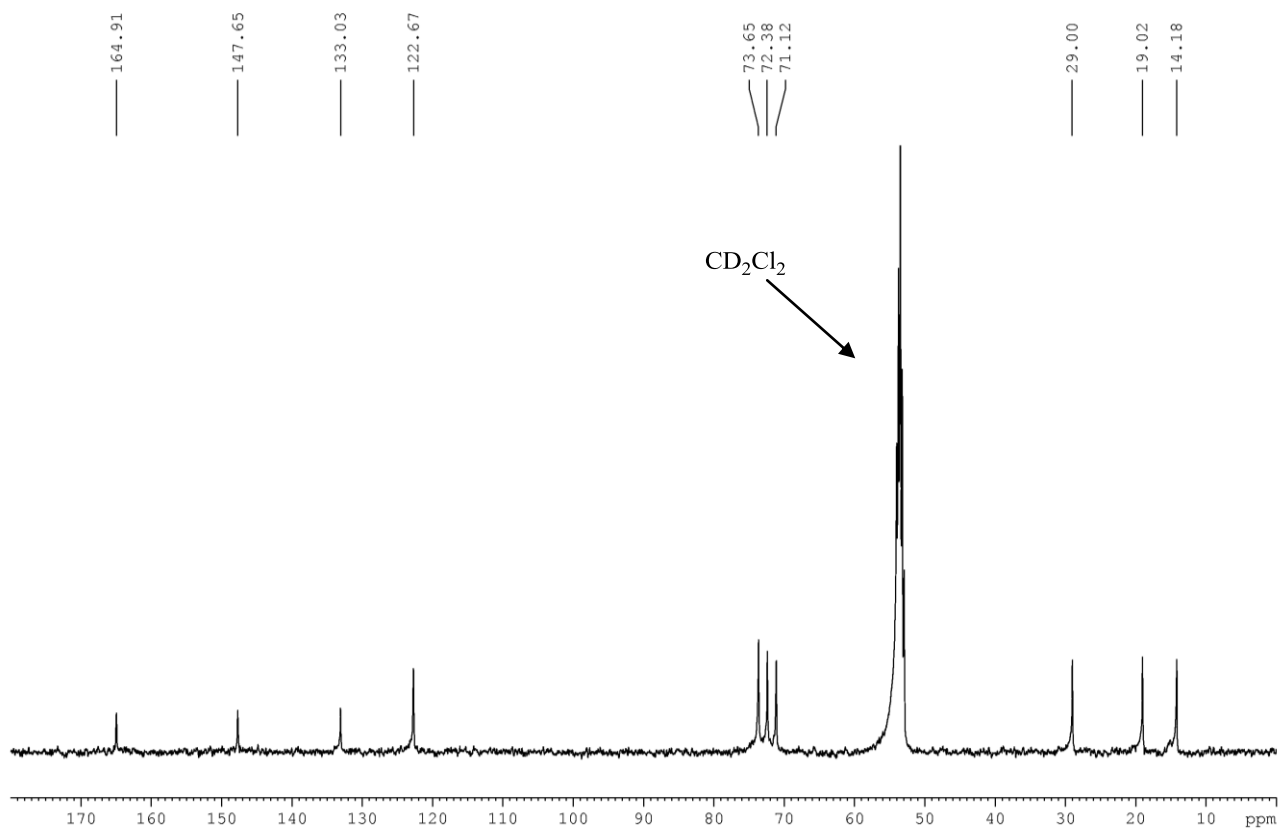
HSQC NMR spectrum (CD_2Cl_2 , 298 K, AV400) of complex **5a**



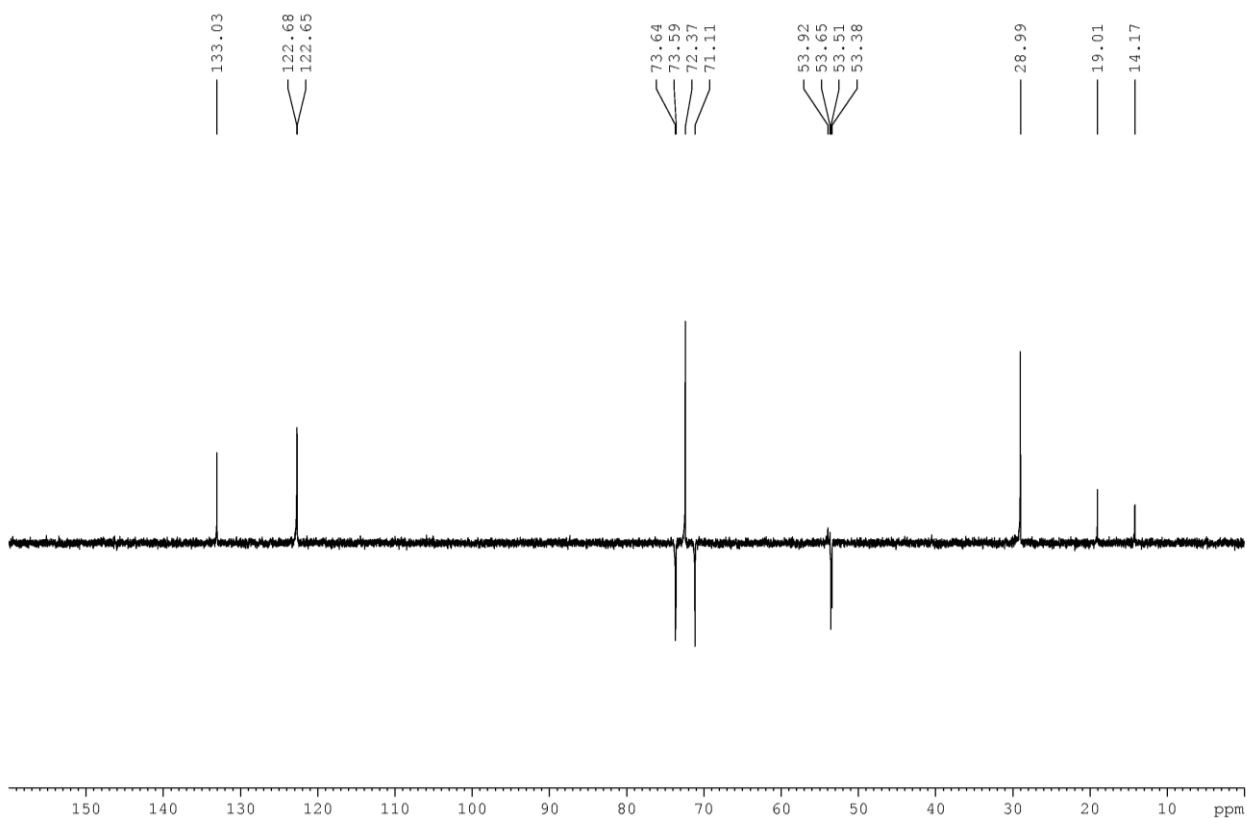
¹H NMR spectrum (CD₂Cl₂, 298 K, AV400) of complex **1b**



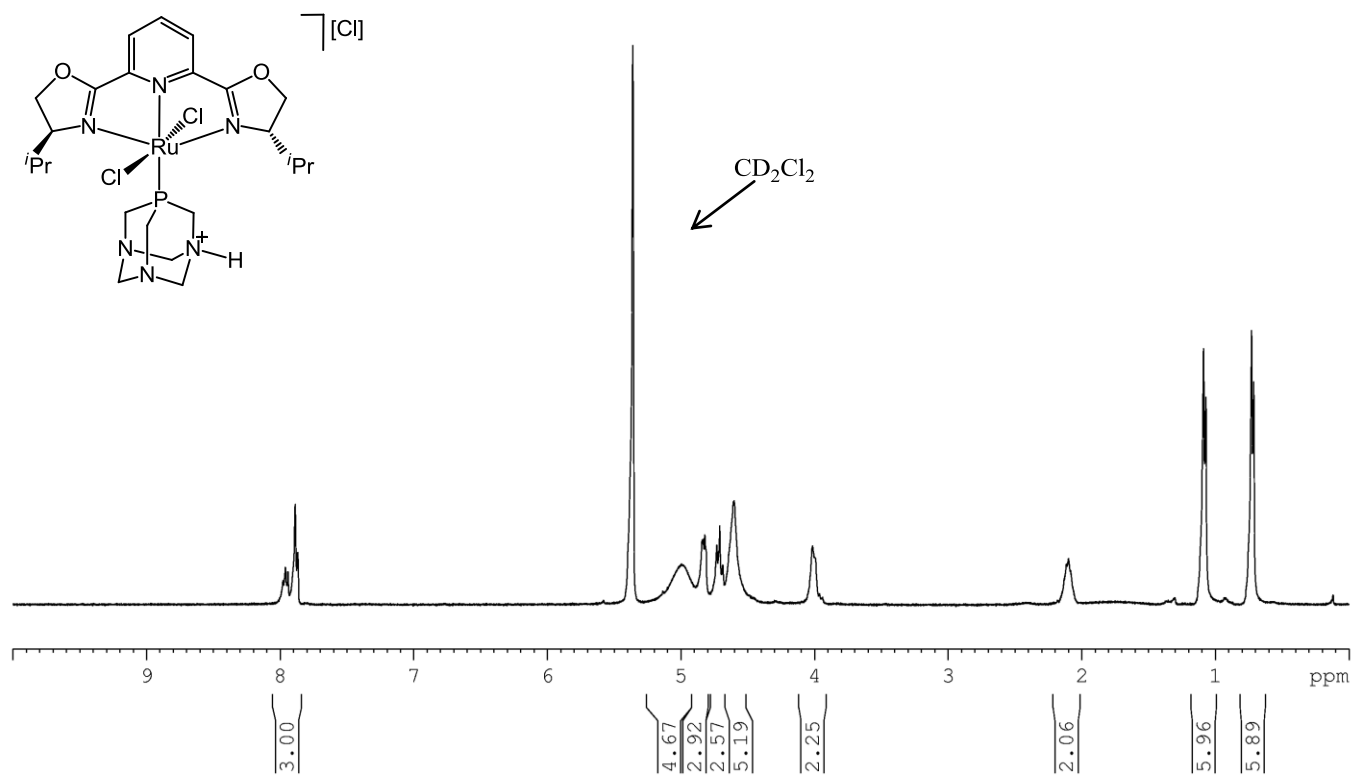
³¹P NMR spectrum (CD₂Cl₂, 298K, AV400) of complex **1b**



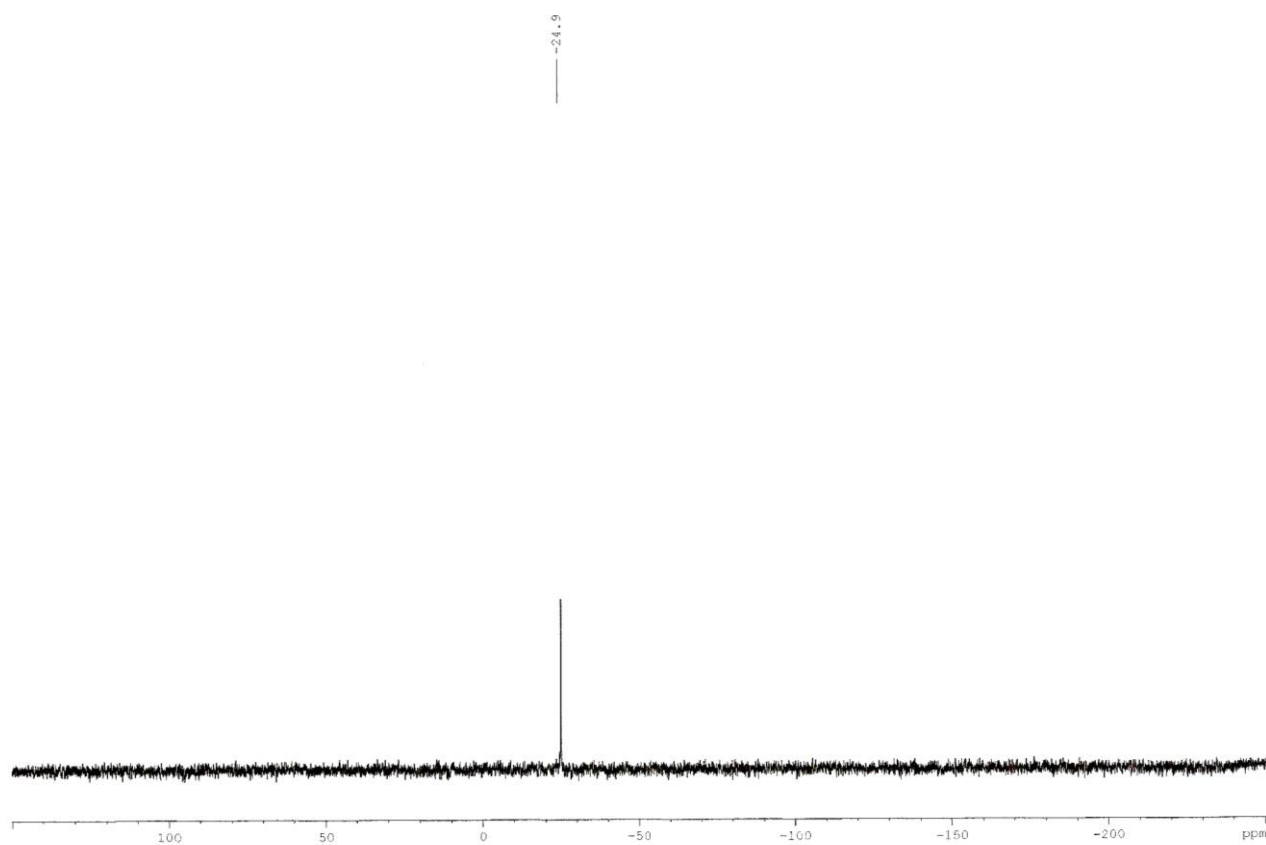
¹³C NMR spectrum (CD₂Cl₂, 298 K, AV400) of complex **1b**



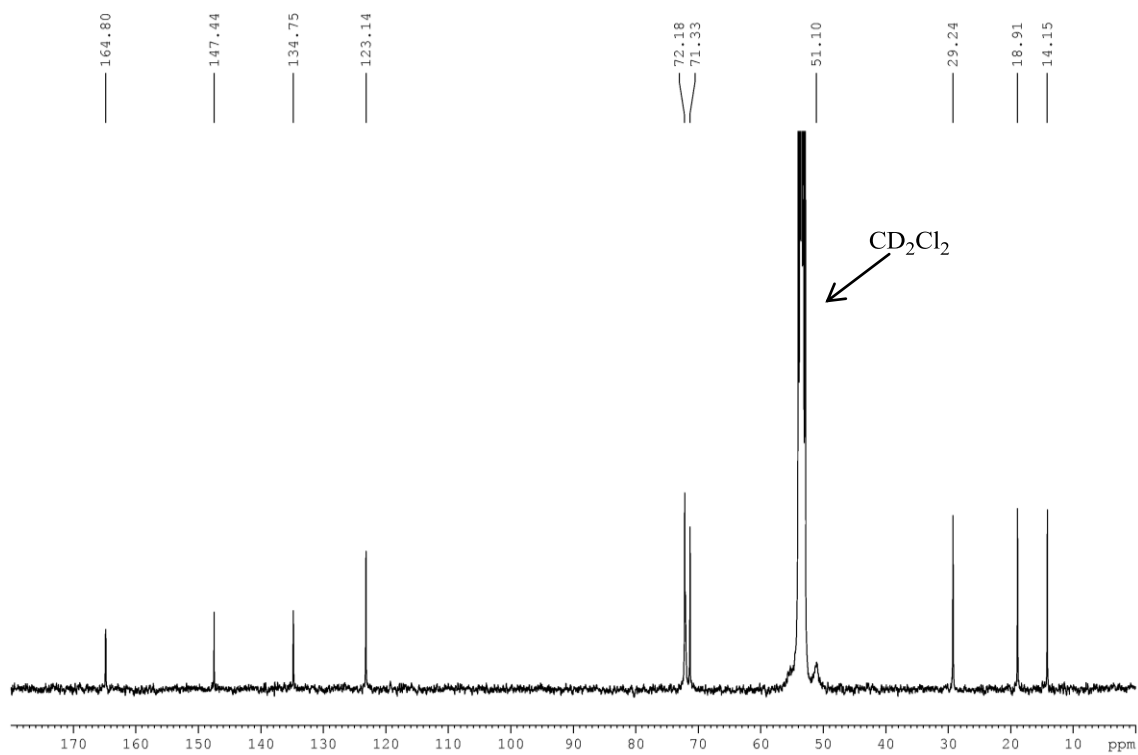
DEPT-135 NMR spectrum (CD₂Cl₂, 298 K, AV400) of complex **1b**



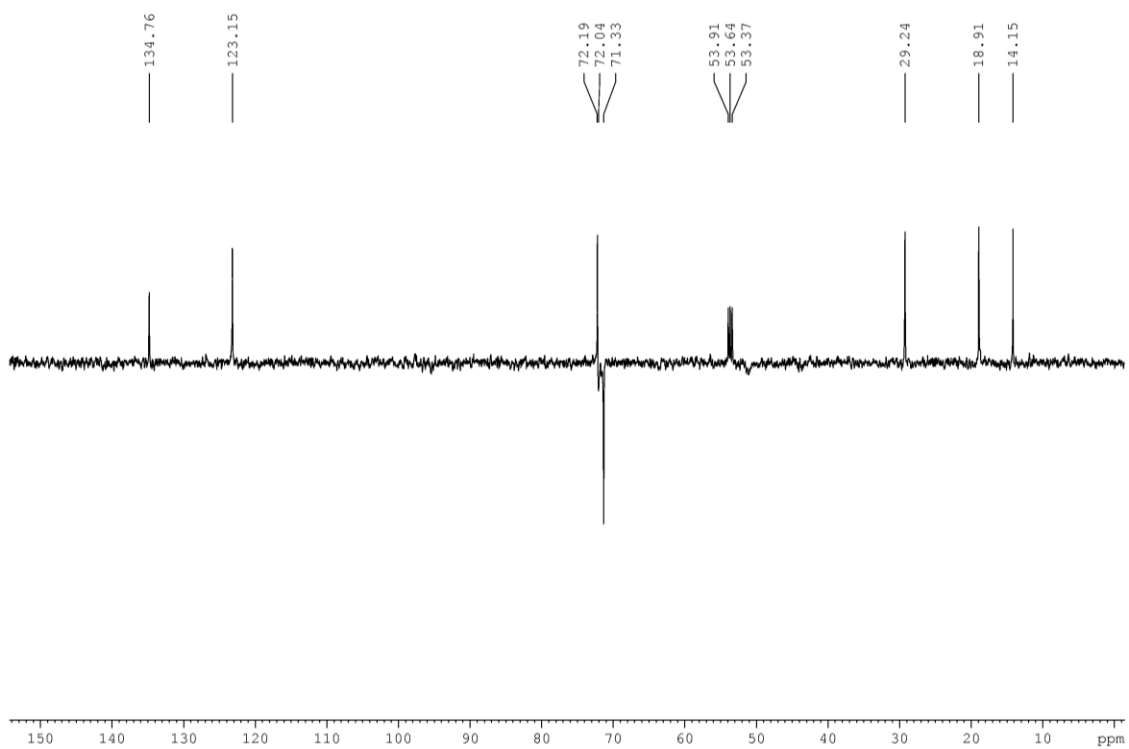
^1H NMR spectrum (CD_2Cl_2 , 298 K, AV400) of complex **2b**



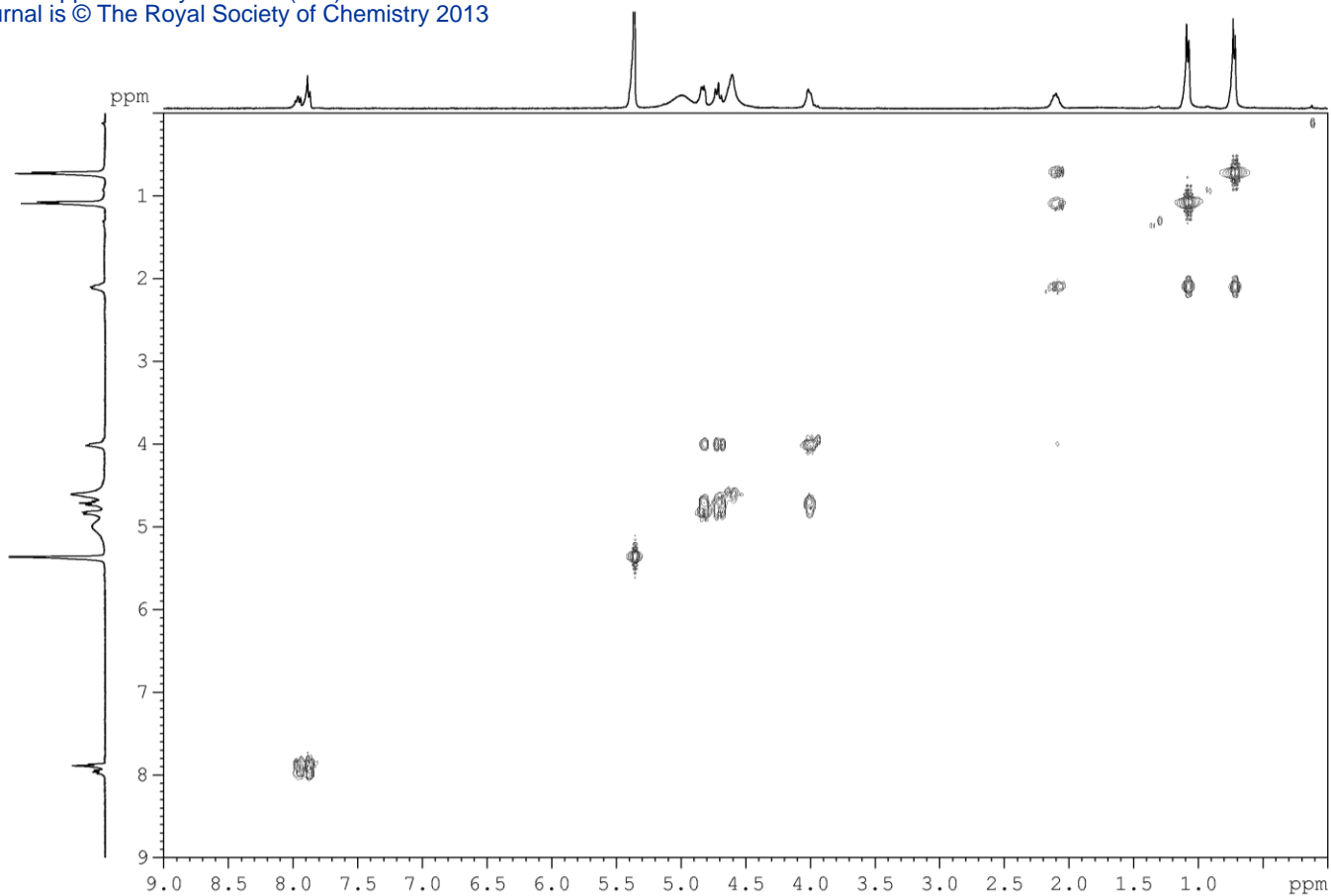
^{31}P NMR spectrum (CD_2Cl_2 , 298 K, AV400) of complex **2b**



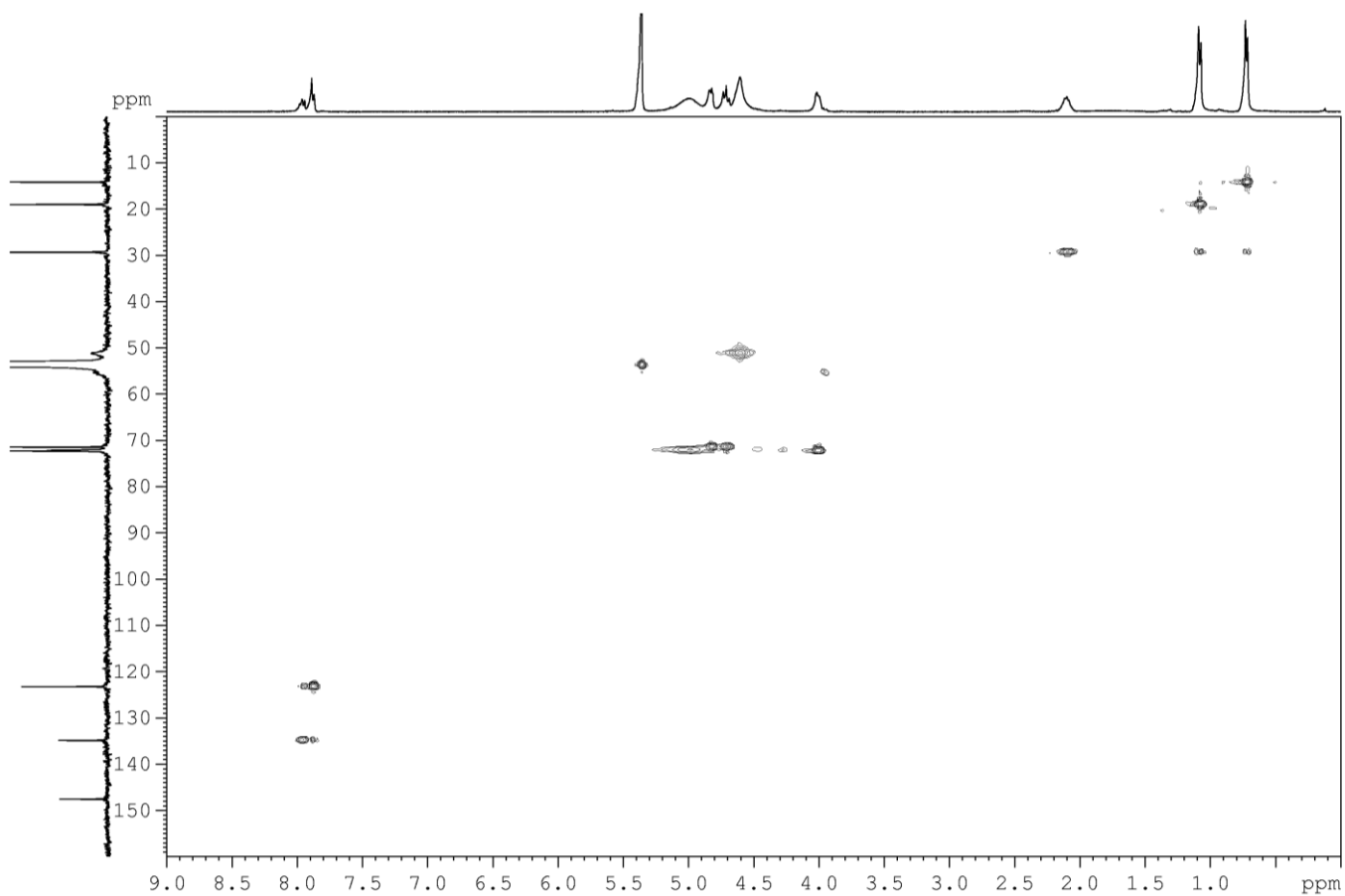
^{13}C NMR spectrum (CD_2Cl_2 , 298 K, AV400) of complex **2b**



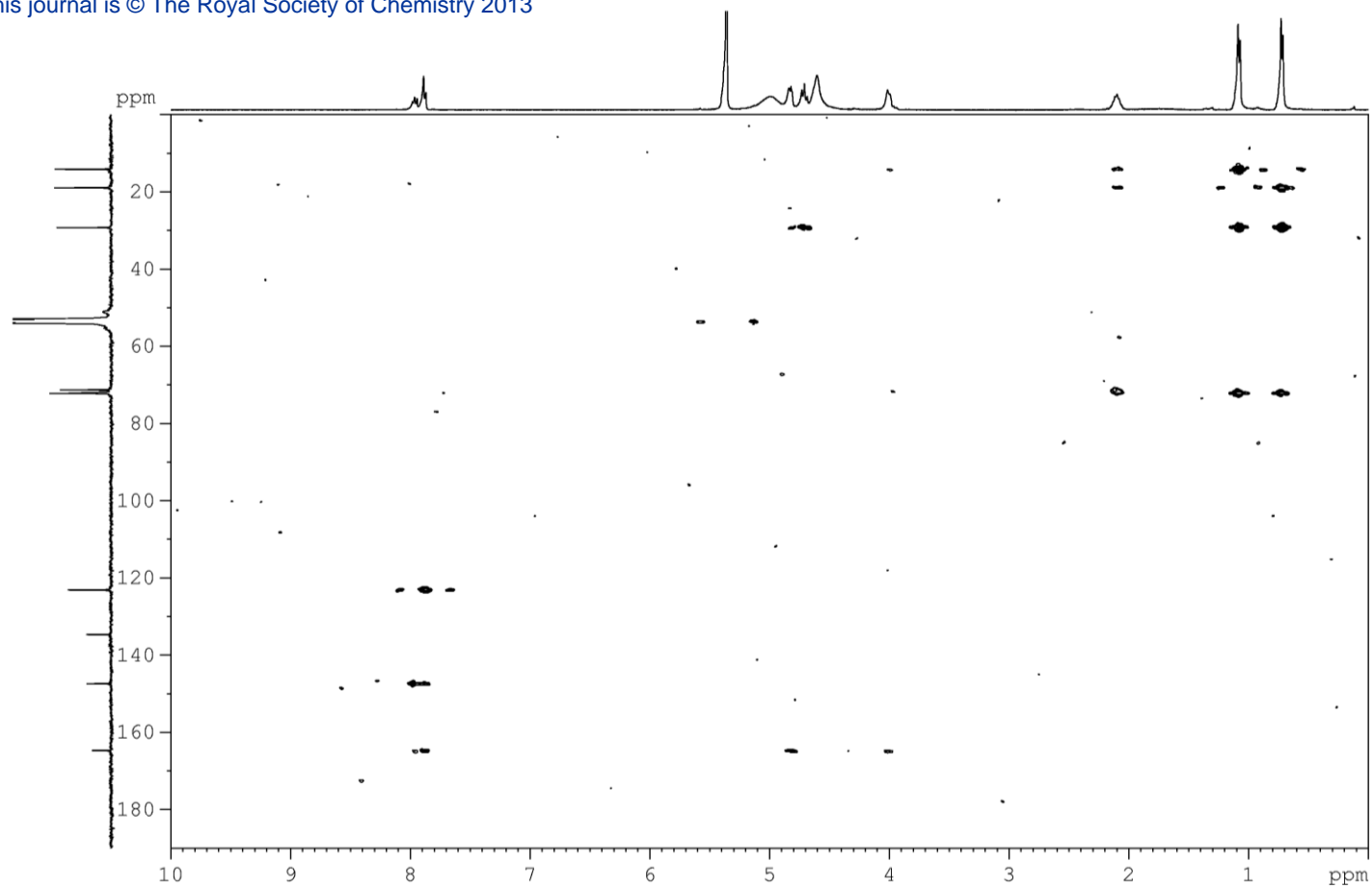
DEPT 135 NMR spectrum (CD_2Cl_2 , 298 K, AV400) of complex **2b**



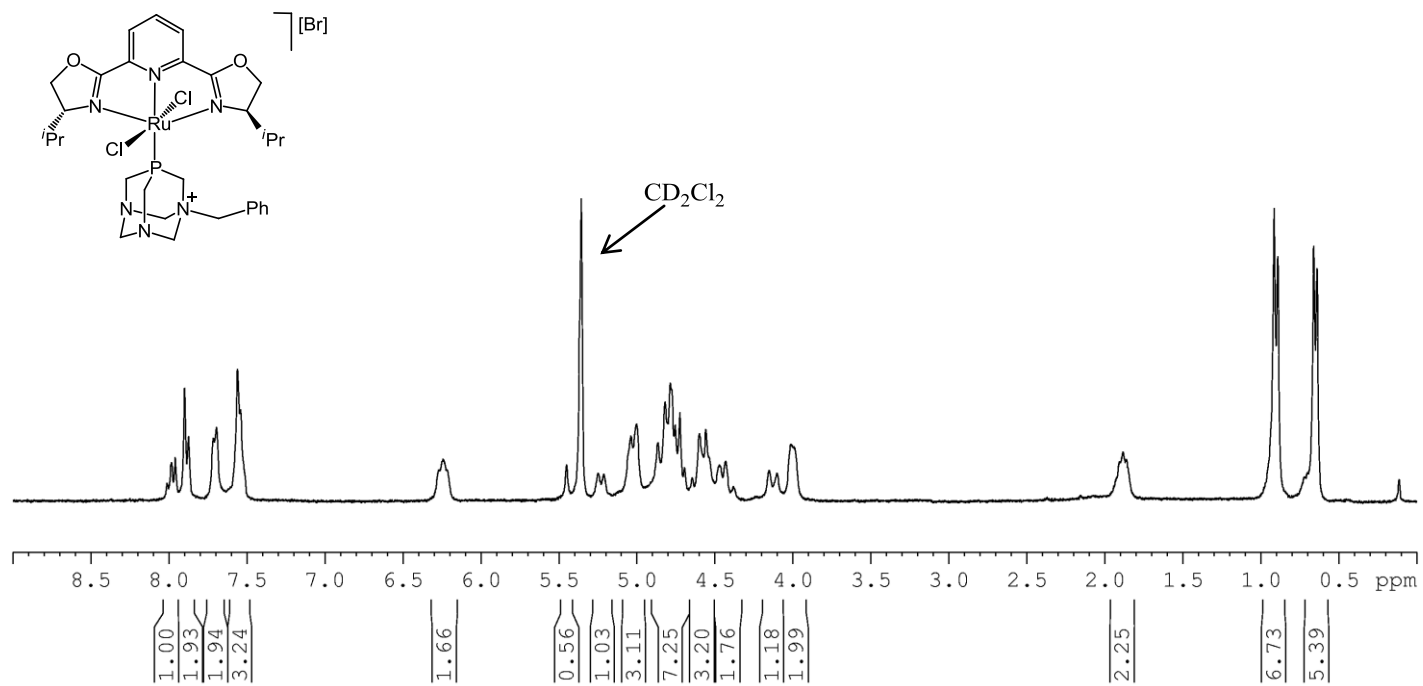
COSY HH NMR spectrum (CD₂Cl₂, 298 K, AV400) of complex **2b**



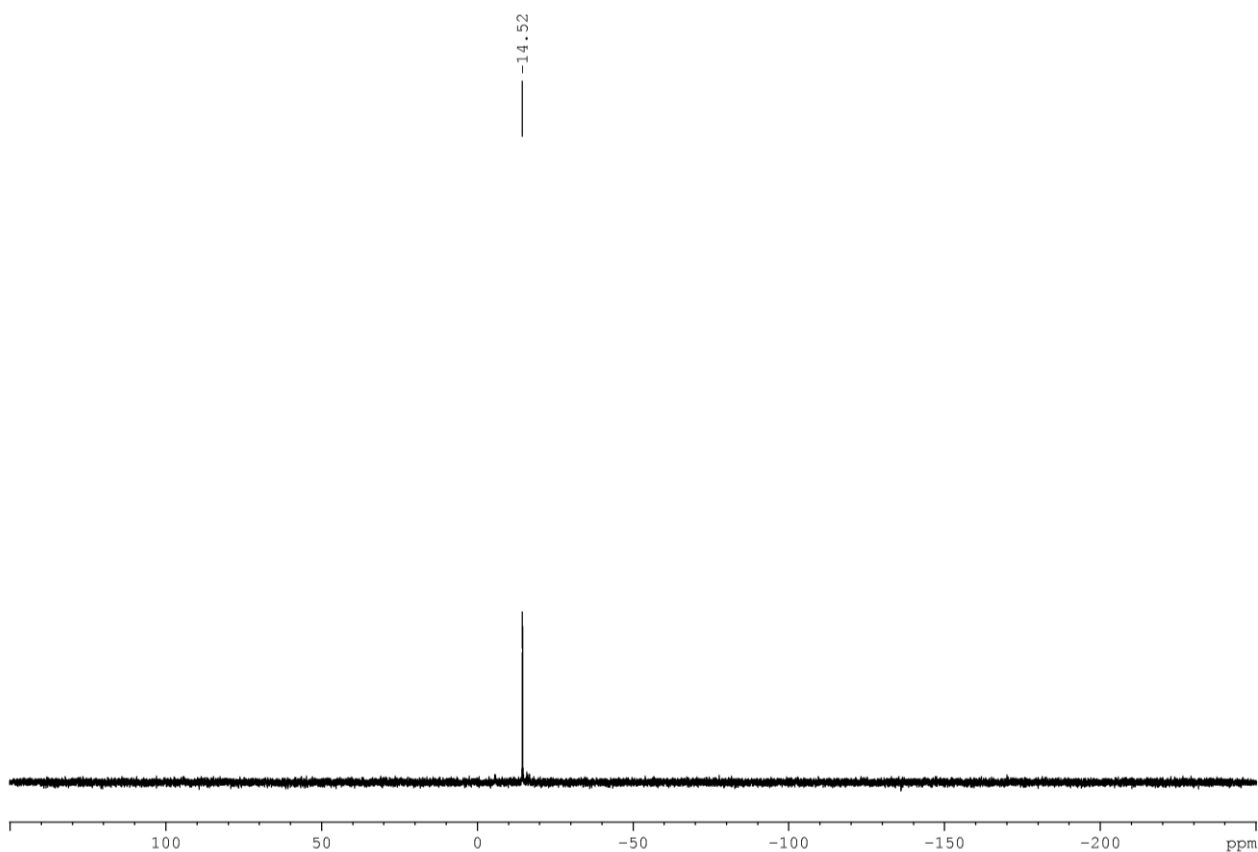
HSQC NMR spectrum (CD₂Cl₂, 298 K, AV400) of complex **2b**



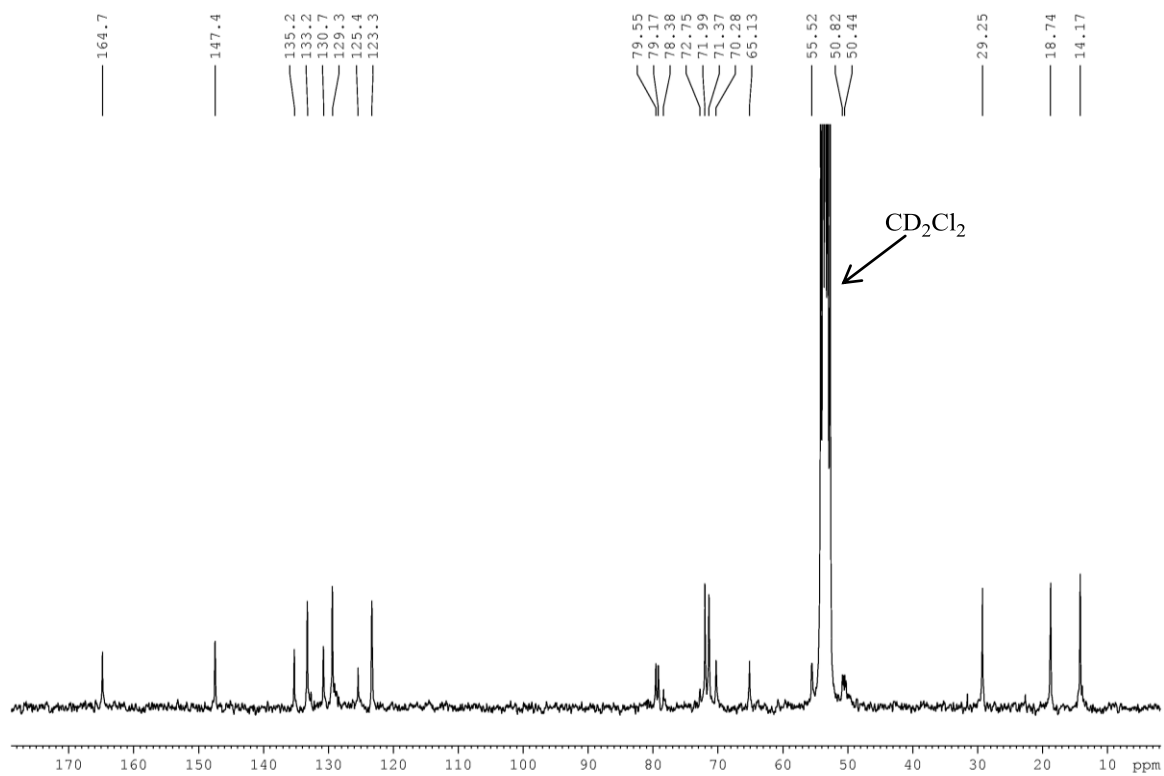
HMBC NMR spectrum (CD₂Cl₂, 298 K, AV400) of complex **2b**



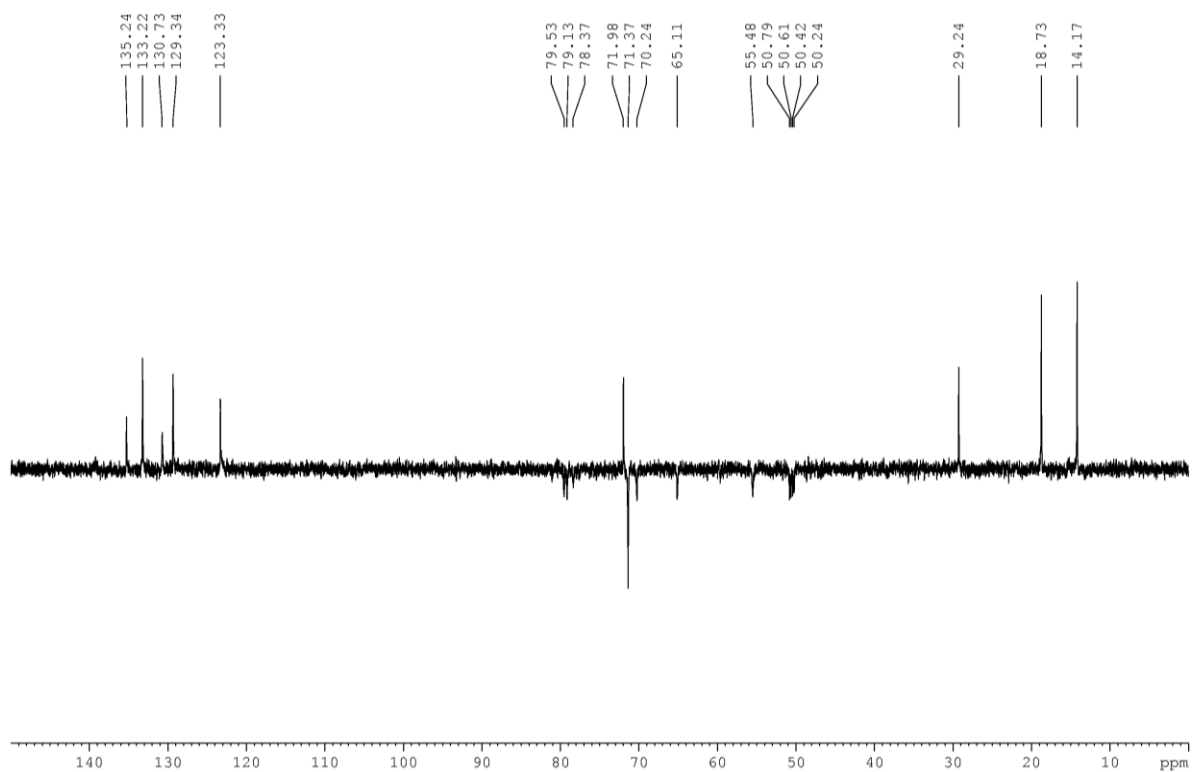
^1H NMR spectrum (CD₂Cl₂, 298 K, DPX300) of complex **6c**



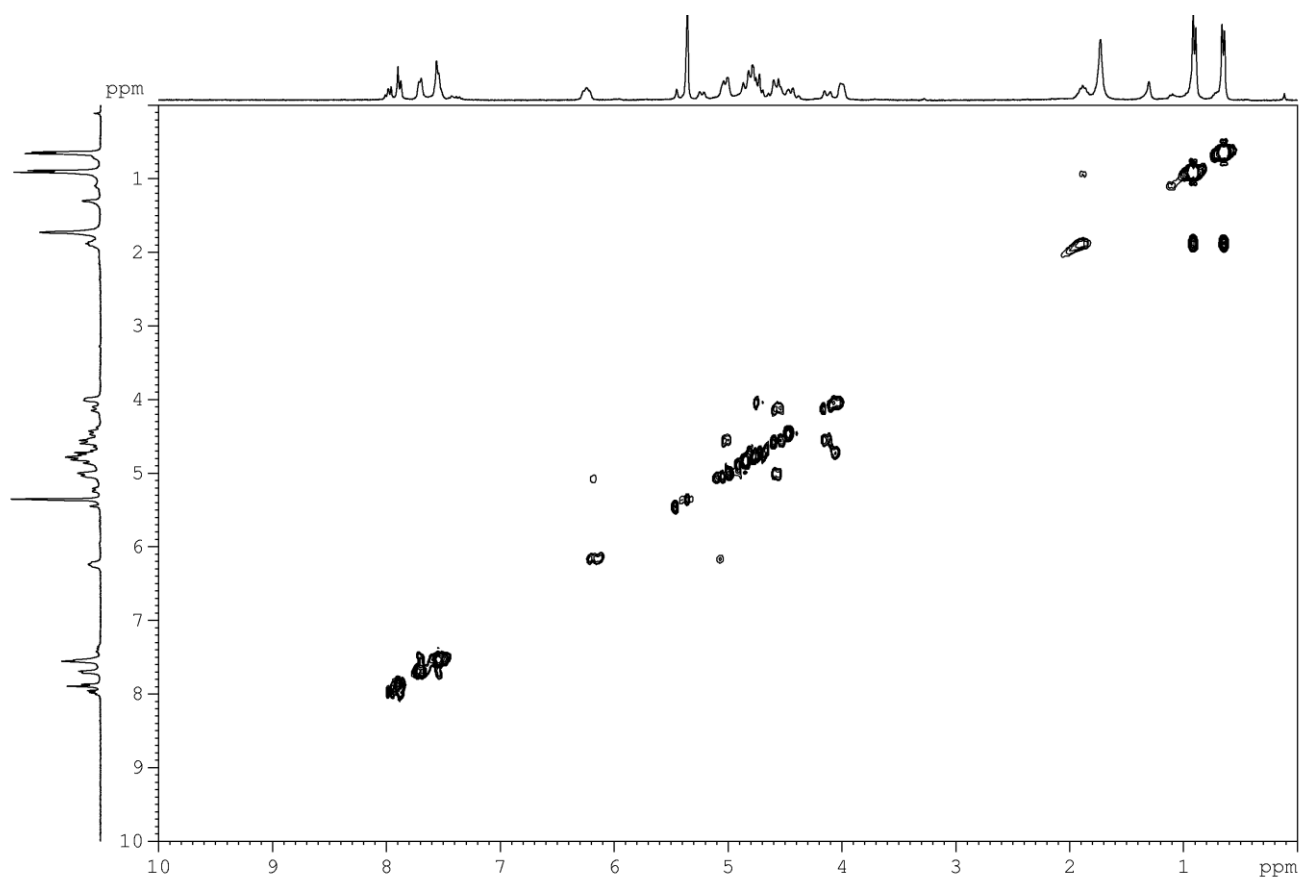
^{31}P NMR spectrum (CD₂Cl₂, 298 K, DPX300) of complex **6c**



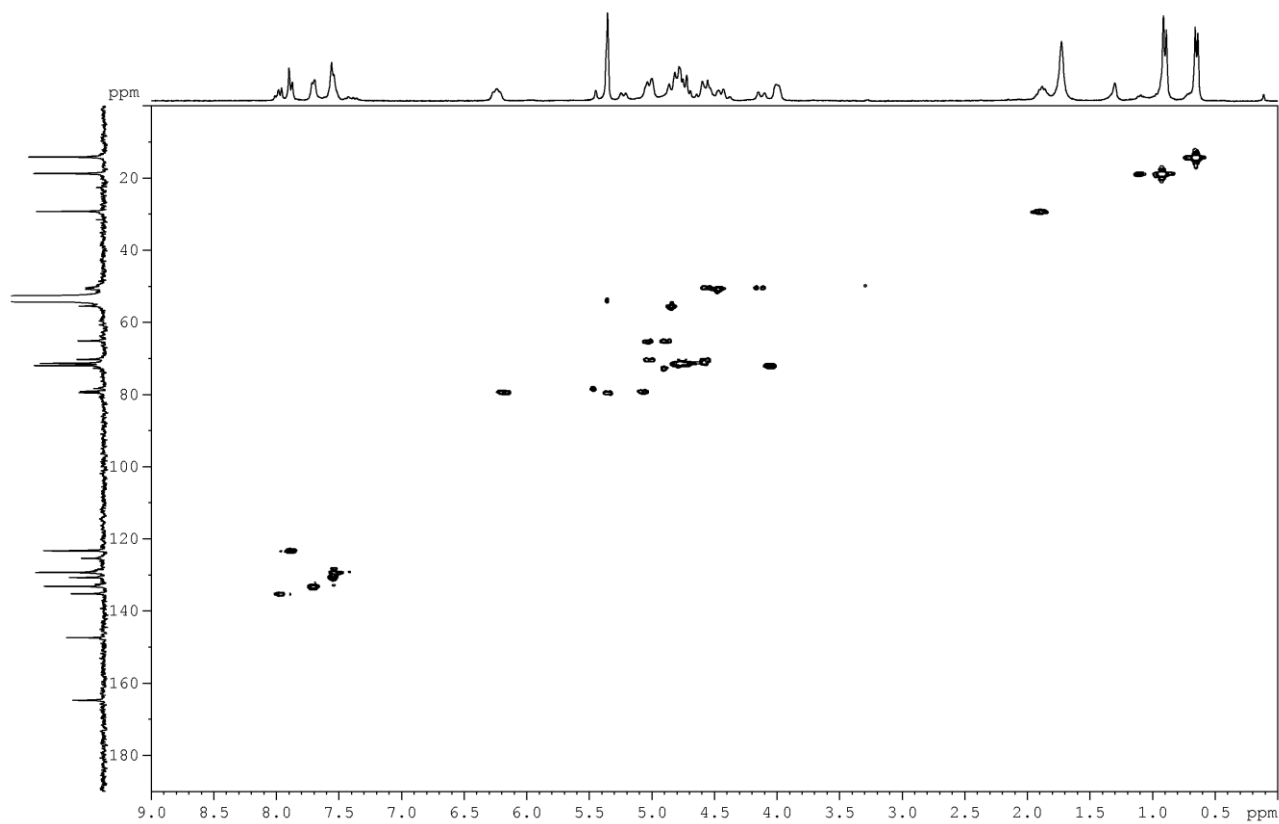
^{13}C NMR spectrum (CD_2Cl_2 , 298 K, AV300) of complex **6c**



DEPT-135 NMR spectrum (CD_2Cl_2 , 298 K, AV300) of complex **6c**



COSY HH NMR spectrum (CD₂Cl₂, 298 K, AV300) of complex **6c**



HSQC NMR spectrum (CD₂Cl₂, 298 K, AV300) of complex **6c**

Antimicrobial Activity.

Experimental

Microbial cytotoxicity of ruthenium compounds was measured against two yeasts (*Candida albicans* ATCC 14053 and *Candida parapsilosis*), and different bacteria: *Micrococcus luteus* ATCC 9341, *Bacillus subtilis* ATCC 19659, *Escherichia coli* C600 ATCC 23724, *Streptomyces coelicolor* A3(2), *Streptomyces antibioticus* ATCC 11891, *Streptomyces glaucescens* DSM 40716 and *Pseudomonas aeruginosa* PAO1 ATCC 15692. The antimicrobial activity was tested according to the Kirby Bauer disc diffusion method [20]. The microorganisms were mixed at known concentrations with Mueller Hinton and poured into petri dishes (9 cm in diameter; 10 mL of culture medium per plate). The ruthenium complex was pipetted onto sterile filter paper disks (0.5 cm in diameter) and the solvent evaporated before placing them on the cultures. Plates were maintained at 4°C during 1 hour, and then incubated at 30°C for the yeasts and *Streptomyces*, and 37 °C for the rest of bacteria. Different amounts per disc were used depending of the compound solubility [355 µg (**1a**), 310 µg (**2a**), 255 µg (**3a**), 160 µg (**4a**), 360 µg (**5a**), 255 µg (**6a**), 595 µg (**1b**), 430 µg (**2b**), 395 µg (**3b**), 530 µg (**4b**), 400 µg (**5b**), 530 µg (**6b**), 530 µg (**1c**), 1090 µg (**2c**), 355 µg (**3c**), 475 µg (**4c**), 430 µg (**5c**), 545 µg (**6c**)]. For the compounds that were effective against microbes the size of the growth inhibition halos was measured in mm.

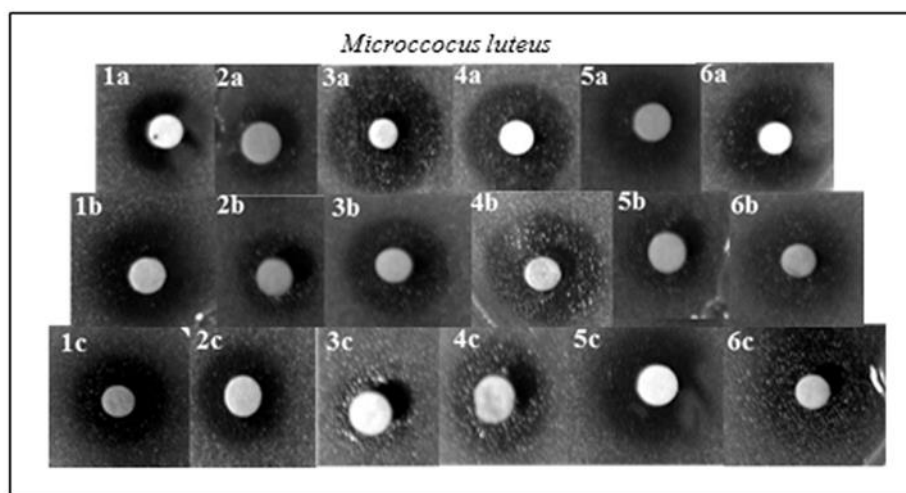


Figure 1. DNA antimicrobial activity of the ruthenium complexes against *Micrococcus luteus*. Ruthenium complex used per disc: 355 μg (**1a**), 310 μg (**2a**), 255 μg (**3a**), 160 μg (**4a**), 360 μg (**5a**), 255 μg (**6a**), 595 μg (**1b**), 430 μg (**2b**), 395 μg (**3b**), 530 μg (**4b**), 400 μg (**5b**), 530 μg (**6b**), 530 μg (**1c**), 1090 μg (**2c**), 355 μg (**3c**), 475 μg (**4c**), 430 μg (**5c**), 545 μg (**6c**).

Table 1: Inhibition halos (mm) of the ruthenium complexes against different microorganisms.

Compound ^a		<i>Micrococcus luteus</i>	<i>Bacillus subtilis</i>	<i>E. coli</i> c600	<i>Streptomyces coelicolor</i>	<i>Streptomyces antibioticus</i>
<i>trans</i> -[RuCl ₂ {(R,R)-Ph-pybox}(PTA)]	1a	12	7	-	-	7
<i>trans</i> -[RuCl ₂ {(S,S)- ⁱ Pr-pybox}(PTA)]	1b	17	15	-	13	11
<i>trans</i> -[RuCl ₂ {(R,R)- ⁱ Pr-pybox}(PTA)]	1c	17	14	-	9	10
<i>trans</i> -[RuCl ₂ {(R,R)-Ph-pybox}(1-H-PTA)][Cl]	2a	14	6	5	-	6
<i>trans</i> -[RuCl ₂ {(S,S)- ⁱ Pr-pybox}(1-H-PTA)][Cl]	2b	15	6	-	-	8
<i>trans</i> -[RuCl ₂ {(R,R)- ⁱ Pr-pybox}(1-H-PTA)][Cl]	2c	15	10	-	-	10
<i>trans</i> -[RuCl ₂ {(R,R)-Ph-pybox}(1-CH ₃ -PTA)][I]	3a	27	7	5	27	22
<i>trans</i> -[RuCl ₂ {(S,S)- ⁱ Pr-pybox}(1-CH ₃ -PTA)][I]	3b	19	9	-	12	20
<i>trans</i> -[RuCl ₂ {(R,R)- ⁱ Pr-pybox}(1-CH ₃ -PTA)][I]	3c	13	8	-	-	10
<i>trans</i> -[RuCl ₂ {(R,R)-Ph-pybox}(1-CH ₂ =CHCH ₂ -PTA)][I]	4a	21	6	5	9	13
<i>trans</i> -[RuCl ₂ {(S,S)- ⁱ Pr-pybox}(1-CH ₂ =CHCH ₂ -PTA)][I]	4b	21	8	-	17	20
<i>trans</i> -[RuCl ₂ {(R,R)- ⁱ Pr-pybox}(1-CH ₂ =CHCH ₂ -PTA)][I]	4c	17	10	-	10	14
<i>trans</i> -[RuCl ₂ {(R,R)-Ph-pybox}(1-HC≡CCH ₂ -PTA)][Br]	5a	17	6	-	6	12
<i>trans</i> -[RuCl ₂ {(S,S)- ⁱ Pr-pybox}(1-HC≡CCH ₂ -PTA)][Br]	5b	13	7	-	-	8
<i>trans</i> -[RuCl ₂ {(R,R)- ⁱ Pr-pybox}(1-HC≡CCH ₂ -PTA)][Br]	5c	19	10	-	-	13
<i>trans</i> -[RuCl ₂ {(R,R)-Ph-pybox}(1-PhCH ₂ -PTA)][Br]	6a	20	7	-	17	13
<i>trans</i> -[RuCl ₂ {(S,S)- ⁱ Pr-pybox}(1-PhCH ₂ -PTA)][Br]	6b	18	8	-	11	13
<i>trans</i> -[RuCl ₂ {(R,R)- ⁱ Pr-pybox}(1-PhCH ₂ -PTA)][Br]	6c	18	14	-	6	11

^aRuthenium complex used per disc: 355 µg (**1a**), 310 µg (**2a**), 255 µg (**3a**), 160 µg (**4a**), 360 µg (**5a**), 255 µg (**6a**), 595 µg (**1b**), 430 µg (**2b**), 395 µg (**3b**), 530 µg (**4b**), 400 µg (**5b**), 530 µg (**6b**), 530 µg (**1c**), 1090 µg (**2c**), 355 µg (**3c**), 475 µg (**4c**), 430 µg (**5c**), 545 µg (**6c**).

Crystal and refinement data for complexes **1b**, **2a·CH₂Cl₂** and **3b**

Table 2. Crystal Data and Structure Refinement for Complexes **1b**, **2a·CH₂Cl₂** and **3b**

	1b	2a·CH₂Cl₂	3b
Empirical formula	C ₂₃ H ₃₅ Cl ₂ N ₆ O ₂ PRu	C ₃₀ H ₃₄ Cl ₅ N ₆ O ₂ PRu	C ₂₄ H ₃₈ Cl ₂ IN ₆ O ₂ PRu
Formula weight	630.51	819.92	772.45
Temperature (K)	293(2)	293(2)	293(2)
Wavelength (Å)	1.5418	1.5418	1.5418
Crystal system	Orthorhombic	Monoclinic	Orthorhombic
Space group	<i>P</i> 2 ₁ 2 ₁ 2 ₁	<i>P</i> 2 ₁	<i>C</i> 222 ₁
<i>a</i> (Å)	11.7278(1)	10.5635(1)	13.5047(2)
<i>b</i> (Å)	12.5536(1)	14.7654(1)	23.2490(5)
<i>c</i> (Å)	18.5962(2)	11.8752(1)	24.3739(4)
<i>A</i> (deg)	90	90	90
<i>β</i> (deg)	90	107.283(1)	90
<i>γ</i> (deg)	90	90	90
Volume (Å ³)	2737.85(4)	1768.60(3)	7652.7(2)
<i>Z</i>	4	2	8
$\rho_{\text{calculated}}$ (Mg m ⁻³)	1.530	1.540	1.341
μ (mm ⁻¹)	7.246	7.797	11.540
<i>F</i> (000)	1296	832	3088
Crystal size (mm ³)	0.046 x 0.04 x 0.02	0.145 x 0.06 x 0.008	0.13 x 0.081 x 0.039
θ range (deg)	4.25 to 73.85	3.90 to 73.97	3.63 to 74.01
Index ranges	-14 ≤ <i>h</i> ≤ 13 -14 ≤ <i>k</i> ≤ 15 -23 ≤ <i>l</i> ≤ 19	-12 ≤ <i>h</i> ≤ 7 -17 ≤ <i>k</i> ≤ 10 -14 ≤ <i>l</i> ≤ 14	-15 ≤ <i>h</i> ≤ 15 -26 ≤ <i>k</i> ≤ 28 -29 ≤ <i>l</i> ≤ 26
No. of reflns. collected	15044	6937	10478
No. of independent reflns.	5210 [R(int) = 0.0429]	4524 [R(int) = 0.0399]	6104 [R(int) = 0.0260]
Completeness to θ_{max} (%)	99.7	99.4	91.7
Refinement method	Full-matrix least-squares on <i>F</i> ²	Full-matrix least-squares on <i>F</i> ²	Full-matrix least-squares on <i>F</i> ²
No. of parameters/restraints	320/0	419/3	325/0
Goodness-of-fit on <i>F</i> ²	1.093	1.103	1.108
<i>R</i> ₁ [<i>I</i> > 2σ(<i>I</i>)] ^a	<i>R</i> ₁ = 0.0364, <i>wR</i> ₂ = 0.0998	<i>R</i> ₁ = 0.0376, <i>wR</i> ₂ = 0.0974	<i>R</i> ₁ = 0.0502, <i>wR</i> ₂ = 0.1395
<i>R</i> (all data)	<i>R</i> ₁ = 0.0443, <i>wR</i> ₂ = 0.1168	<i>R</i> ₁ = 0.0441, <i>wR</i> ₂ = 0.1160	<i>R</i> ₁ = 0.0555, <i>wR</i> ₂ = 0.1446
Absolute structure parameter	0.020(11)	0.022(15)	0.015(15)
Largest diff. peak and hole (e Å ⁻³)	0.592 and -0.678	1.031 and -0.841	1.287 and -0.683

^a $R_1 = \sum(|F_o| - |F_c|)/\sum|F_o|$; $wR_2 = \{\sum[w(F_o^2 - F_c^2)^2]/\sum[w(F_o^2)^2]\}^{1/2}$.